Biomineralization: Elemental and Organic Influence in Carbonate Systems

M. Cusack*,[†] and A. Freer[‡]

Department of Geographical & Earth Sciences and Department of Chemistry, University of Glasgow, Glasgow, Scotland, United Kingdom
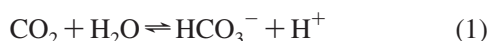
Contents

1. Introduction

The basic building blocks available to evolution when deciding skeletal structure could be summarized in the following equations:

$$CO_2 + H_2O \rightleftharpoons HCO_3^- + H^+ \quad (1)$$

$$Ca^{2+} + HCO_3^- \rightleftharpoons CaCO_3 + H^+ \quad (2)$$

or

$$Ca^{2+} + HPO_4^{2-} \rightleftharpoons CaHPO_4 \quad (3)$$

(as hydroxyapatite, $Ca_{10}(PO_4)(OH)_2$) This dichotomy was resolved when vertebrates evolved utilizing phosphate and

(most) invertebrates evolved utilizing carbonate. So, it would seem that a rather limited amount of skeletal architecture would propagate from such limited design material—how many ways can one diversify calcium carbonate or phosphate? This could not be further from reality where Nature has utilized these fundamental building blocks to create a staggering diversity of structures in the carbonate zone (Figure 1) and continuing evolutionary masterpieces in the vertebrates. The secret to this diversity is the inclusion of organic material (protein, carbohydrate, lipid) as the thread to stitch together complicated structures from a simple cloth. In essence, this is biomineralization.

Biomineral structures perform a range of interrelated functions including support and mobility in the vertebrate skeleton; protection in bivalves, brachiopods (Figure 1D), and foraminifera; embryonic protection in the avian eggshell (Figure 1C); balance in fish otoliths; and detection of the Earth's magnetic field in magnetotactic bacteria (Figure 1B). Directly, or indirectly, the architecture of these biominerals is often crucial to other aspects of existence, e.g., photosynthesis in coccoliths where the calcite plates surrounding the single algal cells (Figure 1A) scatter light,[1−3] protecting the cells from intense UV radiation while the cells compensate for this by increasing chlorophyll *a* production.[4] Another light-related example is photoreception in brittlestars, which is achieved via calcite photoreceptors[5] (Figure 2). Fiber-optical properties have been discovered in siliceous "glass" sponges,[6] where this phenomenon is a function of the layered organic—glass composite structure.[7]

There are at least 60 different minerals in the biosphere.[8] Of these, calcium phosphate, calcium carbonate, and silica are the most abundant. The variety of biomineral ultrastructures and chemical compositions, in combination with the organic components, ultimately determines the physical and material properties of these biocomposites, facilitating the specific functions. The organic components influence the mineral even at the level of the unit cell, where organic components can cause anisotropic lattice swelling.[9] An elegant example of chemical composition facilitating function can be found in the mineralogy of trilobite eyes. Trilobites are an extinct group of arthropods. Schizochroal trilobites eyes are constructed solely of the mineral calcite. Aberration-free vision from such primitive lenses was achieved by small differences in magnesium concentration between the lens and bowl of the trilobite eye[10,11] (Figure 3).

An example where physical properties are enhanced and function is being driven by elemental composition is in the high concentrations of magnesium that occur in sea urchin teeth. These are hard and tough and, therefore, suited for rock scraping during feeding. These robust biomineral structures also serve as an example of the interrelationship between organic and inorganic components in biominerals,

* To whom correspondence should be addressed. Fax: +44 (0)141 330 4817. E-mail: Maggie.Cusack@ges.gla.ac.uk.
[†] Department of Geographical & Earth Sciences, University of Glasgow.
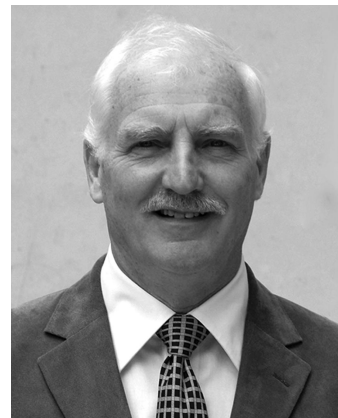[‡] Department of Chemistry, University of Glasgow.

Maggie Cusack graduated with honors in Cell Biology from the University of Glasgow (1985) and progressed to a Ph.D. in Protein Biochemistry from the University of Liverpool (1989) investigating the structure−function of the sweet protein, *Thaumatin*. The protein aspects of biominerals attracted Maggie back to Glasgow in 1989, this time to Geosciences, where she initially worked on modern brachiopod shells. This work led to a highly productive 15 year collaboration with the late Sir Alwyn Williams and a Research Fellowship from the Royal Society of London (1991−1999). In 1999 Dr. Cusack was appointed Lecturer; in 2002 she was appointed Senior Lecturer; and she was appointed Professor of Biomineralisation in 2007. In 2008, she was awarded the Saltire Society Scottish Science Award for 2007. Professor Cusack's research includes many facets of biominerals including trace element and isotope composition in climate recording, crystallography, material properties, and organic−inorganic interactions. Although Professor Cusack continues to work on brachiopods, her research portfolio also includes many invertebrate phyla. Recent funding from the Medical Research Council has enabled Professor Cusack to cross the shell−bone divide and apply her knowledge of invertebrate carbonate biominerals to investigations of bone disease.

Andy Freer was born and raised in Glasgow, Scotland. He became a graduate of the Royal Society of Chemistry (1976) and was awarded his Ph.D. in theoretical crystallography in 1980 from the University of Glasgow. Postgraduate studies during the 1980s on the structure elucidation of important small-to-intermediate sized pharmaceuticals saw a natural transition to protein crystallography in 1989. In 2006, Dr. Freer was elected Fellow of the Royal Society of Chemistry. His main interests lay in the structure determination of membrane proteins, which was rewarded with the structure of the light-harvesting antennae complex, LH2, solved in 1994. Current projects involve the transmembrane proteins from CNS myelin and proteins involved in biomineralization. Promoted to Senior Lecturer in 2000, Dr. Freer strongly believes that, concurrent with a dynamic research profile, it is important to encourage young students to become interested in research, especially at the interface between disciplines.

with the high magnesium concentrations being associated with aspartic acid-rich proteins.[12]

From a geochemistry perspective, there is increasing interest in the stable isotope element composition of biominerals, both of which can be retrieved as proxies for environmental conditions. The stable oxygen isotope composition of brachiopod shell calcite has been used extensively as a seawater temperature proxy, e.g.,[13−15] as has the Sr/Ca ratio of coral aragonite[16,17] and the Mg/Ca ratio of foraminifera.[18,19] The fact that biominerals are produced under strict biological control means that they are not simply passive recorders of their environment. Understanding this biological control, the so-called "vital effect" is required to disentangle biological and environmental influence.

The nature of the crystal lattice will have a *definite* effect on the concentration of trace elements, such as aragonite, accommodating more strontium than calcite and the reverse situation for magnesium.[20] It has long been established that many marine organisms do not simply record seawater composition in the trace and minor element compositions of their biominerals but there is a physiological fractionation that controls the ultimate biomineral composition.[21] Lorens[22] demonstrated the importance of kinetics in influencing the final mineral composition by revealing that the distribution coefficient between the trace element concentration in the crystal (calcite) and the solution decreases with the crystallization rate for Co^{2+}, Mn^{2+}, and Cd^{2+} and increases for Sr^{2+}. Consequently, crystallization rate will influence the final composition of the biomineral. The difficulty in proportioning kinetic effects from the vital effect occurs because biological processes also influence kinetic rates. Physical parameters are also pivotal to the final overall composition and the distribution of trace and minor elements. Within a single polymorph, such as calcite, the effective distribution coefficients for Mg, Mn, and Sr differ by a factor of 7−8 for different faces.[23] Trace element partitioning on {10$\bar{1}$4} faces correspond to crystallographically controlled orientations.[24] The dominant {10$\bar{1}$4} face of calcite contains growth hillocks comprising nonequivalent vicinal faces that partition Mg, Mn, and Sr differently.[25] Mg is more readily incorporated at negative (acute) step edges than in positive (obtuse) edges in calcite when growth is limited by surface reactions. This preference is reversed when growth is limited by diffusion of reactants.[26] In calcite cement crystals, {10$\bar{1}$1} sectors are enriched with Mg and Mn relative to {10$\bar{1}$4}.[27]

Similar differentiation has been recorded in the stable isotope composition of natural calcite crystals with differences between nonequivalent faces of 0.5−2‰ for $\delta^{13}C$ and up to 0.9‰ for $\delta^{18}O$.[28] However, another microsampling study revealed no differences in isotopic composition between sectors.[29] An ion microprobe study of isotopic composition of synthetic calcite indicated that structurally nonequivalent growth steps on a single crystal face do not differ in their fractionation of stable oxygen isotopes.[30] Even in examples where the crystallographic orientation is constant, such as in avian eggshells, the distribution of elements such as magnesium is not homogeneous.[31,32]

Although crystal lattice structure and partition coefficients account for some of the variation in chemical composition found in biominerals, they do not account for the exquisite biological control that leads to such diversity of ultrastructure. There is now accelerating interest in understanding the subtle control exerted by living systems on all aspects of biomineral formation. This research will undoubtedly extend and improve our understanding of biomineralization processes.

Of equal importance is the requirement to determine the elemental and isotopic compositions of biominerals so that we may differentiate biological from environmental factors
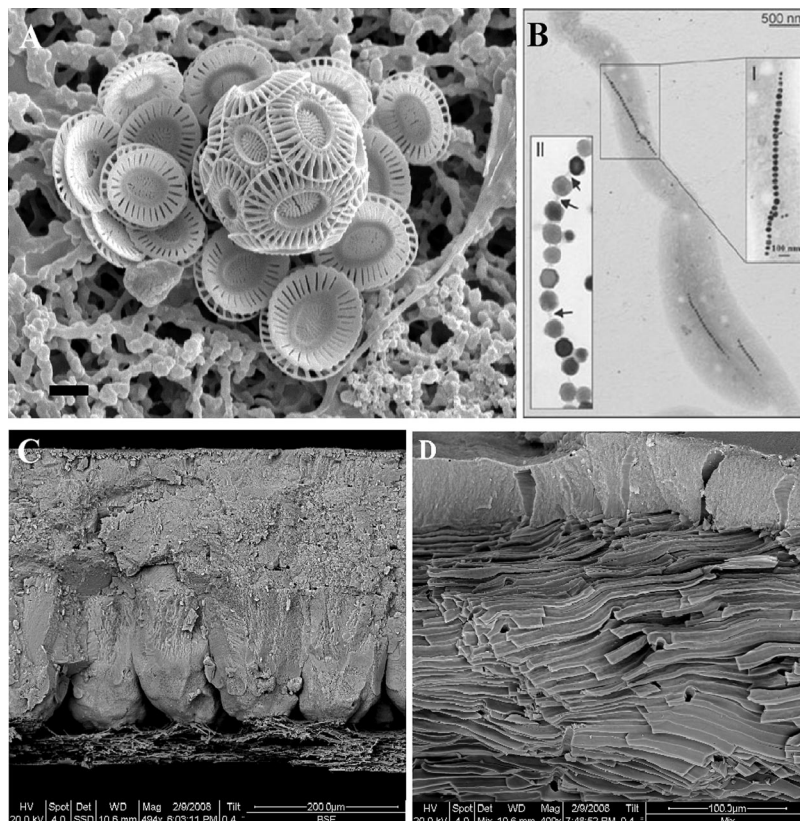
Figure 1. Selection of biomineral structures, each of which performs a specific function. (A) Coccoliths calcite plates on the exterior of a single celled coccolithophorid alga, *Emiliania huxleyi*. Some coccoliths have dropped off, enabling both sides of the coccoliths to be viewed. Scale bar = 1 μm. Coccoliths are thought to provide protection against grazing, improve buoyancy, and scatter light to protect against damage from intense UV as well as improving light capture for species at depth. Reprinted with permission of Jeremy Young. Copyright Natural History Museum, London. (B) Transmission electron micrographs of wild-type *Magnetospiririllum gryphiswaldense* cells. Insets show (I) magnification of magnetosome organization and (II) magnetosome membranes forming junctions (arrows) between isolated crystals from the demonstration that magnetite particles are aligned via an acidic protein, *MamJ*, that is associated with a filamentous structure. Scale bar = 500 nm. Reprinted with permission from ref 290. Copyright 2006 Nature Publishing Group. (C) Backscattered electron image of a fracture section of an eggshell of the domestic fowl, *Gallus gallus*, with shell exterior to top of image and the mammillary caps with membrane on which they nucleated at the bottom of the image. Scale bar = 200 μm. Avian eggshell provides protection for the developing embryo. (D) Mixture of backscattered and secondary electron image of fracture section of *Terebratulina retusa* with outer (primary) layer of acicular calcite toward top of image and underlain by inner (secondary) layer of calcite fibers. Scale bar = 100 μm. Like other shells, the brachiopod shell provides a protected environment for its inhabitant.
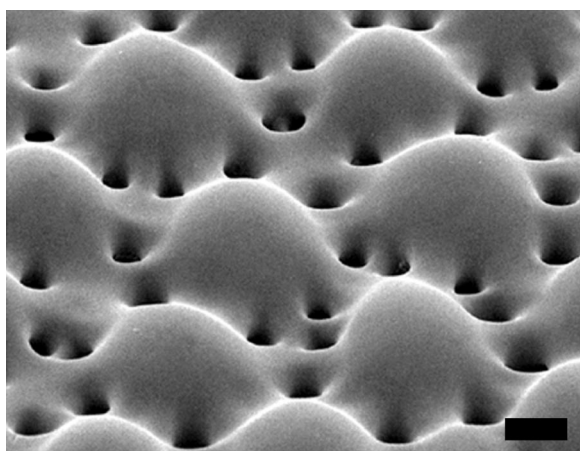

Figure 2. Calcite photoreceptors in the light-sensitive brittlestar, *Ophiocoma wendtii*. Secondary electron image of the peripheral layer of a dorsal arm plate with the enlarged lens structures. Scale bar = 10 μm. Reprinted with permission from ref 5. Copyright 2001 Nature Publishing Group.

in our assignment of trace element and isotope influence. This is an important prerequisite in enabling accurate interpretation of trace and minor elements and stable isotopes

as proxies of environmental information, such as seawater temperature.

In this chapter, we focus on marine invertebrates since they have been studied extensively with a view to understanding and interpreting climate data recorded by their chemical and isotopic composition. The list of carbonate systems considered is extensive but not exhaustive and includes corals, bivalves, brachiopods, coccoliths, and foraminifera.

Although the interest in biominerals as climate proxies dates back more than 50 years,[33-35] it is only recent advances in analytical techniques that have given access to chemical composition at high spatial resolution in the context of structural data. Modern instrumentation, such as secondary ion mass spectrometry (SIMS), wavelength dispersive spectroscopy (WDS), and synchrotron-based analyses such as X-ray absorption near edge spectroscopy (XANES) and X-ray absorption far edge spectroscopy (EXAFS), allows specific data to be collected, often at submicron resolution. Advances in crystallographic techniques such as electron backscatter diffraction (EBSD) enables the extraction of detailed crystallographic orientation data at the same spatial resolution as the isotope and chemical composition, thus contributing to our understanding of the diversity of chemical
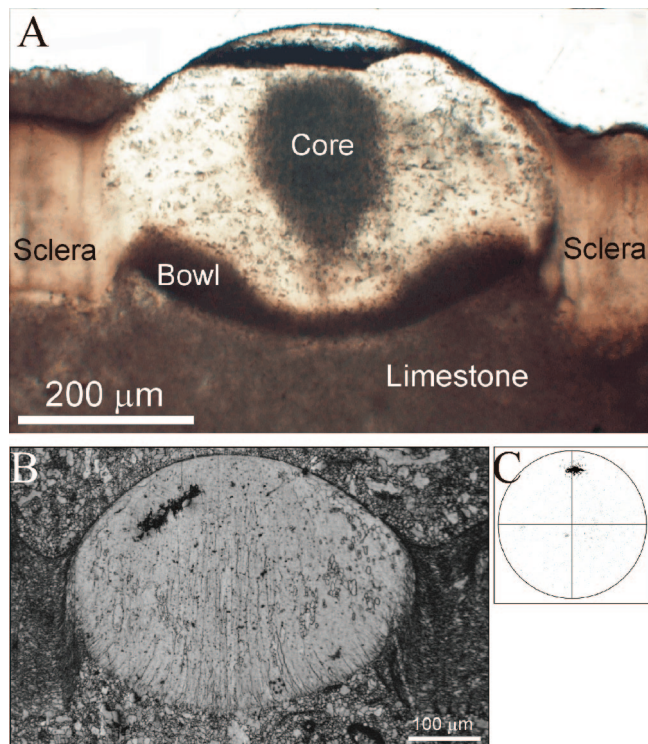
Figure 3. Crystallography of a Schizochroal trilobite eye. (A) Plane polarized transmitted light image of a single lens. Scale bar = 200 μm. (B) Electron backscatter diffraction (EBSD) intensity map of a single lens, with the cornea uppermost, sclera, and enclosing limestone. Scale bar = 100 μm. (C) Pole figure of lens calcite showing the orientations of the poles to calcite {0001} planes (i.e., the c-axis). The pole figure indicates that the c-axis is orientated north–south with respect to the diffraction intensity map and almost in the plane of the thin section. The tight clustering of data points shows that the degree of variation in crystallographic orientations of lens calcite is very limited. Reprinted with permission from ref 10. Copyright 2007 The Palaeontological Association.

composition and the relationships between chemistry, structure, and crystallography.

2. Amorphous Calcium Carbonate

No review of chemico-structural relationships in biominerals would be complete without mention of amorphous calcium carbonate (ACC). It is now very well established that many organisms such as echinoderms,[36-38] crustaceans,[39] and molluscs[40] employ ACC as a transient phase in biomineral development. An ACC layer has been detected around aragonite nacre tablets.[41,42] The coexistence of calcite and ACC in distinct domains within biomineral structures occurs in calcareous sponges and ascidians, organisms that are phylogenetically distant from each other.[43] The transient amorphous phase of sea urchin larval spicules does not have bound water,[37] while stable ACC ($CaCO_3 \cdot H_2O$) contains 15% water.[44] Calcium carbonate may be deposited as a hydrated form and then dehydrated at crystallization.[38] In terms of chemico-structural relationships, the association of magnesium with ACC is highly relevant here. Biogenic ACC contains more magnesium than the corresponding crystalline phase (e.g. in ascidians, ACC and calcite contain 5.9 and 1.7 mol % Mg, respectively[45]), and the same pattern is observed in synthetic ACC,[46] including that grown by the polymer-induced liquid precursor (PILP) method where poly-(α,β)-D,L-aspartic acid is included in the crystallization system.[47] Occluded Mg increases stability of synthetic ACC
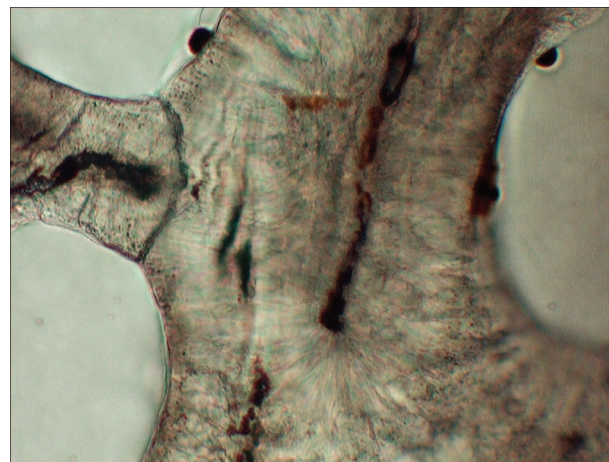
Figure 4. Light microscopy image of *Porites lutea* with aragonite fibers radiating from centers of calcification (dark regions). Field of view = 300 μm. Image from Jenny England and Paul Dalbeck (University of Glasgow).

and in turn influences the crystalline phases developed.[46] Macromolecules from sea urchin larval spicules, together with magnesium ions, mediate the transient formation of ACC as a precursor to calcite.[37] Asprich, an acidic protein from the mollusc *Atrina rigida*, induces and stabilizes the formation of ACC in vitro.[48] It is suggested that Asprich thus stabilizes ACC and controls crystallization into the growing prisms of the *Atrina rigida* shell.[48] Thus, by controlling the chemistry of ACC, organisms control crystal morphology to high fidelity. Nacre has been produced by a retrosynthetic method using the insoluble organic matrix of *Haliotis laevigata* and aspartic acid to stabilize the ACC.[49] Polymorph selection may even occur at this initial amorphous phase since ACC possesses the nascent order of the polymorph that will be produced upon crystallization.[50,51]

3. Corals

Scleractinian or "true" corals produce hard exoskeletons, while the soft corals (*Octocorallia* and *Antipatheria*) may produce calcium carbonate crystals that pervade the soft tissue.[52,53] Details of the structure of scleractinian corals are available in refs 52, 54, and 55. The main aspects of scleractinian architecture are the centers of calcification (COCs) and the fibrous aragonite crystals that radiate from around these centers (Figure 4). The spatial arrangement of the centers and the incremental zonation of the fibers vary between taxa.[56] It has been proposed that coral growth is via two matrix-mediated steps, with the initial mineralization characterized by randomly oriented microgranular components and the second step characterized by consistent crystallographic alignment that determines the crystallography of the aragonite fibers.[57] The centers of calcification have a high organic content[58] in which aragonite crystals are embedded.[58] The crystallinity of the aragonite within the centers may be lower than in the fibers.[56] The fibrous aragonite crystals comprise the bulk of the coral composition and, in contrast to the centers, have a low organic concentration of about 1% by weight[52] while the entire skeleton contains at least 3% by weight organic material.[59]

Annual density banding in corals[60-62] enables the structures to be dated, and thus, the potential for extracting high temporal resolution environmental information from corals is one reason why these living archives are used extensively as climate proxies. Coral aragonite is produced under

biological control, which influences the composition and morphology of coral aragonite.[63] Detailed knowledge of the distribution of trace and minor elements as well as stable isotopes will enhance our understanding of this biological control and also contribute to the accurate interpretation of climate proxies such as Sr/Ca and Mg/Ca ratios, which, in corals, fluctuate systematically yet inversely with $\delta^{18}O$.[64]

3.1. Corals—Organic Components

The most complete study of protein from corals is that of the 53 kDa protein named Galaxin extracted from the exoskeleton of the reef coral *Galaxea fascicularis*.[65,66] A cDNA encoding this protein was cloned, and the primary structure of 298 amino acids was deduced. It has a tandem 30 residue repeat and is glycosylated, but with no apparent calcium-binding activity. Interestingly, there are two conserved dicysteines (Cys-Cys) in each of the 9 repeats that may invoke cross-linking to form a polyprotein network. Two less abundant proteins of approximate masses 45 and 20 kDa, were simultaneously isolated from *G. fascicularis*: neither showed calcium-binding activity. In a similar fashion, 4 proteins have been isolated from *Tubastrea aurea* of approximate masses 70, 53, 46, and 32 kDa, of which the 46 kDa band was the most abundant and likely to be a glycoprotein but not a calcium-binding protein (CaBP).[66] However, the 70 and 53 kDa proteins did show calcium-binding activity and may be involved in the calcification process, perhaps inducing nucleation of $CaCO_3$ crystals. A number of proteins have been isolated from the soluble organic matrix (SOM) of two further scleractinian zooxanthellate corals.[67] *Stylophora pistillata*, a robust branched coral, has yielded 3 acidic proteins of apparent molecular weights (MWs) 55, 47, and 37 kDa, of which only the 55 kDa entity stained positive for calcium-binding. In the leafy complex coral, *Pavona cactus*, 5 acidic proteins were defined from SDS-PAGE analysis of the SOM with apparent MWs 68, 50, 47, 37, and 33 kDa. The proteins of 68, 50, and 47 kDa stained as CaBPs. The amino acid content of the proteins found in the SOM for these two species is consistent with that obtained for other biomineral species.[68−71]

Of particular interest in this study is the long polyaspartate (36 Asp) domain of the 55 kDa protein from *S. pistillata*. It has long been proposed[69,72−74] that this particular sequence denotes control of polymorph outcome, e.g., promoting calcite instead of aragonite. Such poly-L-aspartate sequences, where the negatively charged Asp residues are ideally suited for high-capacity calcium-binding, appear in numerous diverse areas such as the bone matrix proteins, osteopontin[75,76] and aspein,[77] from pearl oyster shells. As well as the proteins recorded for both of *P. pistallata* and *P. cactus*, the presence of the other protagonist in biomineralization—polysaccharides—was also found in relatively high quantities in the SOM. In this instance, *S. pistillata* had a higher proportion (16-fold) of glycosaminoglycans than *P. cactus*, while the percentage of sulfated glycoproteins was similar.

High-performance liquid chromatography (HPLC) investigation of the SOM from two symbiotic scleractinian corals, *Monsastrea curta* and *Porites australiensis*, showed only one main protein at 160 kDa for *M. curta* and one main protein at 200 kDa and a less abundant protein at 25 kDa for *P. australientis*.[59] In both instances, high molecular weight acidic sulfated polysaccharides were found.
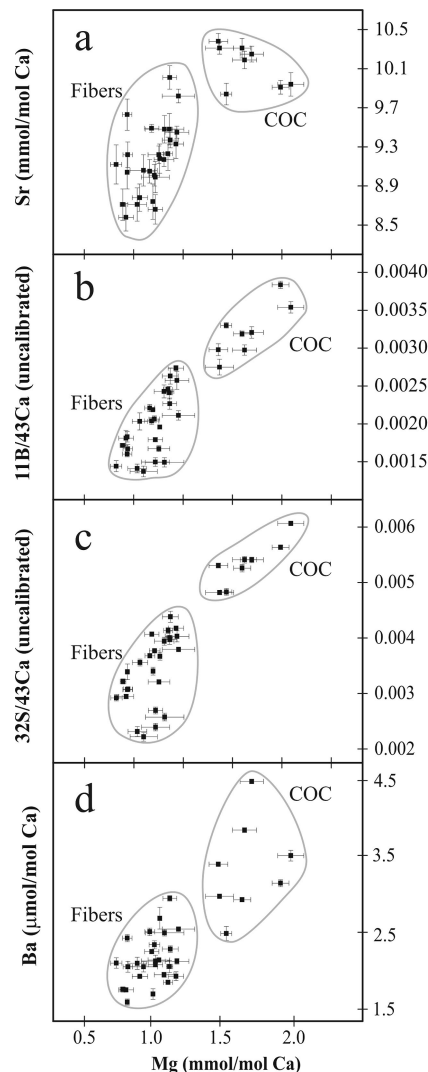

Figure 5. Trace element composition of centers of calcification and fibers of *Colpophyllia sp*. Reprinted with permission from ref 82. Copyright 2006 American Geophysical Union.

3.2. Spicules

Rahman et al.[78,79] studied the organic matrix derived from spicules of two species of alcyonarian coral. In each case, they found a plethora of proteins in the organic matrix. SDS-PAGE analysis of *Synularia polydactyla* showed seven protein bands with apparent molecular masses of 109, 83, 70, 63, 41, 30, and 22 kDa, of which the 109 and 63 kDa fractions tested positive for calcium-binding. Periodic acid Schiff (PAS) staining indicated that the 83 and 63 kDa proteins are glycosylated. A tandem study on spicules from the alcyonarian, *Lobophytum crassum*, isolated 4 proteins from SDS-PAGE with apparent molecular masses of 102, 67, 48, and 37 kDa. The 102 and 67 kDa proteins are calcium-binding proteins, and the 67 kDa protein is glycosylated and rich in acidic amino acids.

## 3.3. Corals—Minor Element Distribution

Distribution of trace and minor elements is not uniform throughout the coral skeleton.[80] The centers of calcification contain higher concentrations of magnesium,[81] strontium, and barium than the fibers[80,82] (Figure 5). Heterogeneity in strontium concentration occurs both within and between the COCs and the fasciculi.[83] Despite this, since strontium
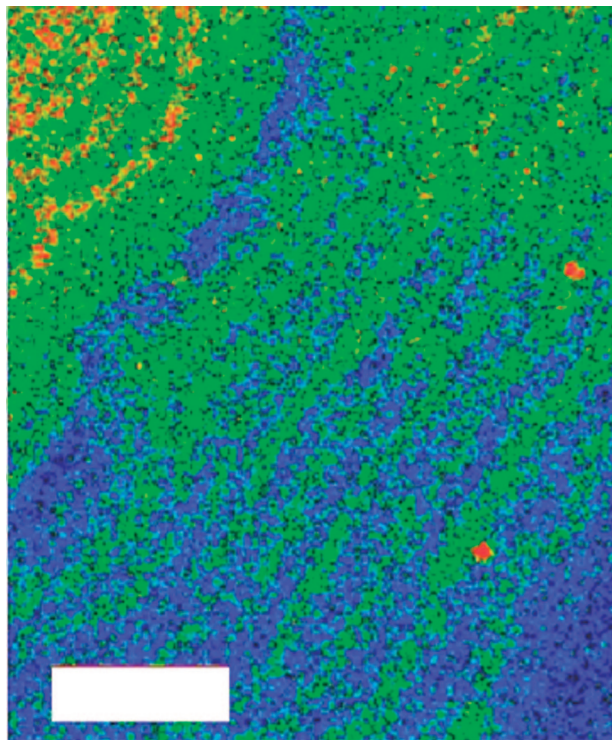
Figure 6. Wavelength dispersive spectroscopy (WDS) map of magnesium distribution in *Pavona clavus* skeleton. Blue indicates relatively low Mg concentrations, and green, yellow, and red correspond to increasingly higher concentrations of magnesium. Scale bar = 10 μm. Reprinted with permission from ref 81. Copyright 2004 American Geophysical Union.

replaces calcium by ideal substitution in scleractinian corals, this simplifies the relationship between the sea surface temperature (SST) and the Sr/Ca ratio, since the free energies of two different phases would result in a more complicated relationship.[83] Monthly oscillations in Sr concentration across the corallite walls of *Porites lutea* are likely to relate to spawning and larval release and may explain difficulties in obtaining accurate seawater temperature data from Sr/Ca ratios.[17] Other factors that may influence strontium concentration and distribution are the activity of symbiont zooxanthellae[84] and tidal modulation.[85] In *Porites lobata*, Mg/Ca ratios are broadly consistent with annual cycles in sea surface temperature, yet there are also interannual fluctuations that are not associated with temperature.[86] Magnesium distribution is different from that of strontium, with changes in magnesium concentration corresponding to the layering in the aragonite fibers[81] (Figure 6). The fact that magnesium concentration in the centers of calcification is >10 times that of the fibers suggests that magnesium concentration is under biological control[81] and that seasonal or subseasonal relationships between water temperature and coral trace element composition may be secondary.[55] Ranges of trace element concentration in deep sea corals where thermal forcing is nil and where they are likely to be driven by biological processes, are of the same range as in *Porites*,[87,88] suggesting that biology may be the driving force for the changes in trace elements in coral skeletons.[55] Synthetic growth experiments indicate that growth rate influences the incorporation of magnesium but not strontium into aragonite, and this may be relevant to biogenic aragonite structures such as corals.[89] This is, however, not in agreement with suggestions that strontium incorporation is influenced by growth rate with the recommendation that Sr/Ca ratios should be determined
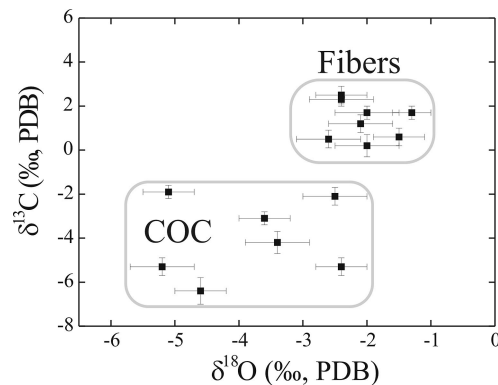
Figure 7. Carbon and oxygen isotope compositions of centers of calcification and fibers of *Colpophyllia sp*. Reprinted with permission from ref 82. Copyright 2006 American Geophysical Union.

in regions of slow growth rate where biological influence is less[17] or from coral aragonite grown at night.[90] A study with cultured Porites species grown at two different temperatures suggests that it is strontium incorporation that is influenced by water temperature while magnesium incorporation is influenced by growth rate.[91] From studies on the massive brain coral, *Diploria labyrinthiformis*, it has been suggested that changes in partitioning of specific elements with changes in temperature, "surface entrapment",[92,93] and seasonal fluctuations in the amount of aragonite precipitated from the calcifying fluid may form the basis of the temperature information recorded in scleractinian corals.[94]

3.4. Corals—Stable Isotope Distribution

The application of $\delta^{18}O$ as a proxy of seawater temperature requires the same consideration of oxygen isotope composition in the context of structure as for minor elements above. Just as there are differences in trace element concentrations between the centers and fibers, so too for stable isotope composition with the centers being lighter in both $\delta^{13}C$ and $\delta^{18}O$ than the fibers[82,95] (Figure 7). The depletion of ^{13}C and ^{18}O in the centers suggest that the calcifying medium in corals has a higher pH[96] than in forams since forams never achieve such ^{13}C and ^{18}O depletions. In *Porites lutea* (zooxanthellate) and *Lophelia pertusa* (azoxanthellate), the heterogeneity in $\delta^{18}O$ correlates with microstructure.[97] The isotopic range may be explained in part by variations in pH.[97,98] In *L. pertusa*, the centers have a narrow range of $\delta^{18}O$ values compared to the fibers, with differences of several per mil over several microns, which suggests specialization of the calicoblastic cell.[97]

4. Foraminifera

Foraminifera are unicellular amoeboid protists that produce a test (shell). They are studied extensively because of their vast abundance in both the planktonic and benthic marine environment and rapid evolution, which makes them important index fossils and contributors to the rock record. Their attractiveness as a source of climate proxies lies in their abundance and ability to produce calcite from seawater trapped within vesicles. Both benthic[99−101] and planktonic[102−104] foraminifera have been employed in studies of past climate.

Details of the evolution of foraminifera are available in the manuscript by Armstrong and Brasier,[105] and details on test formation and composition are in the manuscript by Erez.[106] Foraminifera form four main groups based on
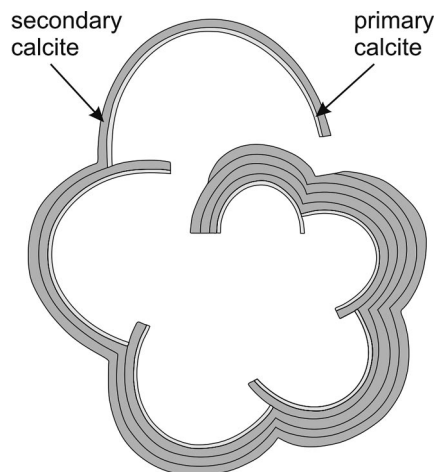
Figure 8. Formation of new chamber and laminate structure in perforate foraminifera. Each new chamber has two layers. The primary calcite outlines the new chamber and becomes the inner lamella. Secondary calcite covers the inner lamella and the entire shell. Reprinted with permission from ref 106. Copyright 2003 Mineralogical Society of America.

diagnostic features of the test: those with organic tests, agglutinated tests ("foreign" particles incorporated into test), imperforate calcite tests, and perforate calcite tests.[106] Perforate calcite tests are the most abundant today and are, therefore, used extensively in climate proxy work and hence are discussed here.

The calcite test consists of a series of chambers that are constructed sequentially. In life, the protoplasm of the cell pervades the chambers and exudes to the exterior of the test, functioning in excretion, food capture, and chamber construction. Assembly of a new chamber wall begins with the protoplasm extending outward to define an outline that extends beyond the position of the proposed chamber. Calcification then takes place within this defined space with the formation of an organic layer or membrane that forms the shape of the new chamber. Nucleation occurs on both sides of this organic template, forming a new layer of primary calcite in the form of a new chamber wall that is then overlain by another layer of (secondary) calcite that extends over the entire test (Figure 8). Thus, the perforate calcite tests become increasingly laminated.

4.1. Foraminifera—Organic Components

Perhaps foraminifera best demonstrate the intimate relationship between the living organism and shell (test). This relationship is realized by the controlled calcification upon and within a preformed organic framework provided by the protoplasm, whereby matrix macromolecules are found within and lining the test. This provides both strength and a biologically preformatted structure to the test.[107] The necessity for a complete functioning mechanism for biomineralization is demonstrated in the study of shell malformation in stressed *Amphistegina*,[108] where anthropogenic stresses and global warming have led to a variety of test damages including test thinning and subsequent breakage due to the lack of internal structural integrity. Comparisons between the organic matrix of damaged and normal tests shows minimal organic material in the damaged tests, which compromises the test architecture. The organelles responsible for protein synthesis (endoplasmic reticulum) and glycosylation (Golgi bodies) are often lacking in damaged *Amphiste-*

gina,[109] resulting in a paucity of glycosaminoglycans, the biomineral building blocks for foraminiferan chambers.

The proteins found in foraminifera appear to fall into two categories that can be isolated by HPLC from a heterogeneous mix of polypeptides.[110−112] One class has high percentages of aspartic and glutamic acids, while the second class is rich in glycine, serine, and alanine. Six species of core-top planktonic foraminifera were investigated by Robbins and Brew,[110] who found a close correlation with the protein analysis on living benthic foraminifera previously carried out by Weiner and Erez.[111] Reverse-phase HPLC showed that the proteins from the six species had comparable chromatographic profiles, indicating that protein composition is similar from species to species.[113] The isolation of a particular protein component, FP8, is likened to the fibrous elastin or silk-fibroin structural proteins where tensile strength and viscoelasticity are required during chamber formation.

Interestingly, a further study of two planktonic foraminifera, *Orbulina universa* and *Pulleniatina obliquiloculata*, showed a protein where the N-terminus region comprised at least 9 aspartic acids in *P. obliquiloculata* and 5 in *O. univera*.[114] Further work on *O. universa* showed 8 proteins of approximate molecular weight 109, 96, 82, 72, 65, 55, 35, and 18.5 kDa. The 65 kDa protein containing a polyaspartic region was isolated.[115] The existence of this polyanionic domain, common to both species, is familiar to the corals where a long polyaspartate (36 Asp) domain of the 55 kDa protein from *S. pistillata* is thought to control polymorph outcome since it is rich in high-capacity calcium-binding sites.

4.2. Foraminifera—Minor Element Distribution

The formation of laminate tests results from striking biological control even in these single-celled organisms. This control extends to the chemical composition of the test. An excellent example of the heterogeneity of minor element distribution in perforate tests comes from in vivo observations of recalcified individuals, where the primary wall contains as much as 12 mol % Mg while the secondary wall comprises up to 3 mol % Mg.[18] This temperature-independent variability of Mg/Ca demonstrates that biology sets the boundaries over which temperature can have influence.[18] In *Globigerina bulloides* and *Globorotalia truncatulinoides*, there is more variation in Mg/Ca ratios than in Sr/Ca ratios between species and between chambers of individual specimens.[116] The low Sr/Ca variability among five species of foraminifera led Elderfield et al.[102] to conclude that seawater temperature is the greatest influence on Sr content in foraminifera tests. The interspecies and intratest variability in Mg concentration, all of which indicate biological control on this parameter, led Bentov and Erez[117] to explore the extent of the biological influence. They proposed a mechanism involving different biomineralization pathways that result in different Mg/Ca ratios. The high Mg-calcite phases may precipitate from transient amorphous calcium carbonate or from the involvement of organic components while the low Mg-calcite precipitates from seawater that is confined and depleted in Mg (Figure 9). By culturing *Amphistegina lobifera* and *Amphistegina lessonii* in culture medium with different Mg concentrations, a positive correlation between Mg concentration in culture media and the resultant test was demonstrated in both species, although *A. lobifera* incorporated greater amounts of Mg than *A. lessonii*.[118] These in vivo experiments reveal the fact that the partition coefficient
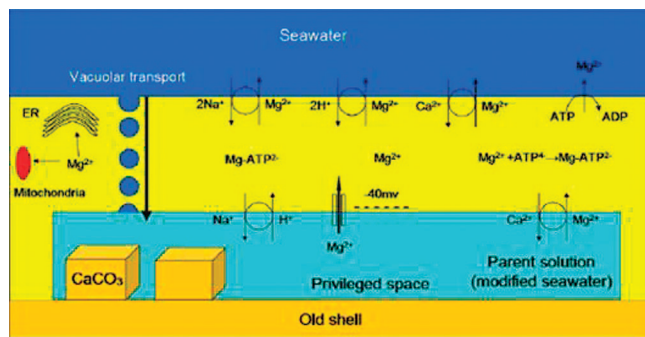
Figure 9. Model for removal of magnesium from seawater during foraminiferan chamber wall formation. Model depicts seawater being delivered to privileged space via vacuoles. Mg^{2+} then moves into the cell via Mg^{2+} channels (bold arrow) courtesy of concentration gradient and membrane potential of $-40mV$. Within the cell, Mg^{2+} is buffered by negatively charged molecules such as adenosine 5'-triphosphate (ATP) as well as sequestration into mitochondria and endoplasmic reticulum. Excess Mg^{2+} is extruded via ion exchangers and pumps. Reprinted with permission from ref 117. Copyright 2006 American Geophysical Union.

of Mg is influenced by the Mg/Ca ratio rather than the Mg^{2+} or Ca^{2+} concentration per se in the culture medium.[118] Despite the heterogeneity of magnesium distribution in the planktonic foraminifera *Pulleniatina obliquiloculata*, the average Mg/Ca ratio does reflect seawater temperature.[119] With larger sample sizes, variability in Mg/Ca and Sr/Ca ratios is much reduced.[116] The higher Mg/Ca and Sr/Ca ratios coincide with the distribution of organic components[119] (Figure 10). Mg concentrations correlate negatively with those of Ca, suggesting ideal substitution of Mg for Ca within the lattice. Mg also correlates well with S as sulfate; only this time, the correlation is positive[106] (Figure 11).

In planktonic foraminifera, Mg/Ca increases linearly with temperature while Sr/Ca decreases and $\delta^{13}C$ increases with increasing specimen size.[120] These trends are considered to be a consequence of growth rate with higher calcification rates in smaller individuals and vice versa. Thus, growth rate influences Mg and Sr composition of foraminifera tests.[120] Techniques such as quadrupole ICP-MS are now available to measure up to nine element/Ca ratios in a single specimen of foraminifera at high spatial resolution.[121] Such an approach is likely to advance our understanding of the relationships between the elements in the context of biomineralization.

Heterogeneity of trace element distribution influences preservation potential[122,123] with Mg content of planktonic foraminifera affecting dissolution susceptibility such that the high Mg-calcite parts of the test may dissolve several hundreds of meters above the low Mg-calcite parts as they approach the carbonate compensation depth (CCD).[122] In the planktonic foraminifera *Globorotalia tumida*, the high Mg-calcite has poorer crystallinity than the low Mg-calcite. More rapid dissolution of the high Mg-calcite results in diagenetic increase in crystallinity.[123]

4.3. Foraminifera—Stable Isotope Distribution

The $\delta^{18}O$ of tests of benthic foraminifera have a constant offset from ambient seawater $\delta^{18}O$, while the $\delta^{13}C$ composition is influenced by microhabitat.[101] Studying the two dominant deep-sea taxa, Corliss et al.[124] demonstrate that, in *Planulina wuellerstorfi*, test $\delta^{13}C$ reflects that of bottom waters, making this taxon useful for reconstructing deep-

ocean circulation, while *Pistominella exigua* $\delta^{13}C$ provides information on productivity and seasonality.[124] In planktonic foraminifera, Mg/Ca ratios tend to follow $\delta^{18}O$ seawater temperatures, although those species living at or near the surface have a higher variation in Mg/Ca ratio than would be predicted from $\delta^{18}O$ seawater temperatures.[120]

5. Coccolithophorids

Coccolithophores are unicellular haptophyte algae that produce elaborate external calcite plates, known as coccoliths (Figure 1A). Coccolith formation occurs within intracellular vesicles with the complete coccolith being extruded to the exterior by fusion of the vesicle and cellular membrane, e.g., ref 125

5.1. Coccoliths—Organic Components

In coccolithophorids, Nature has produced one of her finest and most intricate biomineral designs. All the more remarkable that they should be formed by such efficiency of resources. The assemblage of such structures appears to be accomplished in the main by complexes of acidic polysaccharides that either build the organic framework or backbone for biomineralization or coat the calcite nanocrystals. Controlled biomineralization via acidic sulfated polysaccharides also occurs in other biomineral systems, such as corals[126] and molluscs.[127] The mechanism and role of these coccolith-associated polysaccharides (CAPs) has been studied extensively.[125,128−131]

Coccolith mineralization takes place in two stages: in the first stage, a ring of simple oriented calcite crystals are nucleated about a base plate rim to form a protococcolith. The second stage forms the mature coccolith by transforming the simple ring of crystals into an elaborate double disk of interlocking anvil-shaped calcite. The coccolith precursors—oval organic base plates and acidic polysaccharides—are synthesized in *medial*- and *trans*-Golgi and transferred to the mineralization vesicle.[130]

The mechanism of coccolith formation has largely been gleaned from the study of two species: *Pleurochrysis carterae* and *Emiliania huxleyi*.

In *P. carterae*, three polysaccharides (PS1, PS2, and PS3) are involved in coccolith formation. PS1 and PS2 render an amorphous polysaccharide coat that acts through specific stereochemical alignment of polysaccharide and calcite nanocrystal to adhere in the correct orientation to the base plate rim.[129,132,133] This is the first stage.

In the second stage, a third polysaccharide, named PS3 in *P. carterae* and coccolith polysaccharide in *E. huxleyi*, is a sulfated galacturonomannan[128,134] that is involved directly in shaping the calcite rim but not in the initial nucleation of the mineral phase and formation of the protococcolith ring. The definition of the role of PS3 was determined by the study of a *P. carterae* mutant that has no PS3 expression.[130]

The dominant role in coccolith biomineralization played by CAPs is unusual since, in most biomineralization systems, proteins play a key role. To date, there has been a dearth of proteins isolated from the shell structure of coccoliths; the only example is the protein named GPA (glutamic acid-proline-alanine), which was deduced from the nucleotide sequence.[135] GPA has a remarkable composition, containing 24% acidic residues and high proline and alanine contents, which makes it homologous to the acidic calcium-binding proteins. Furthermore, GPA has a 35 amino acid repeat,
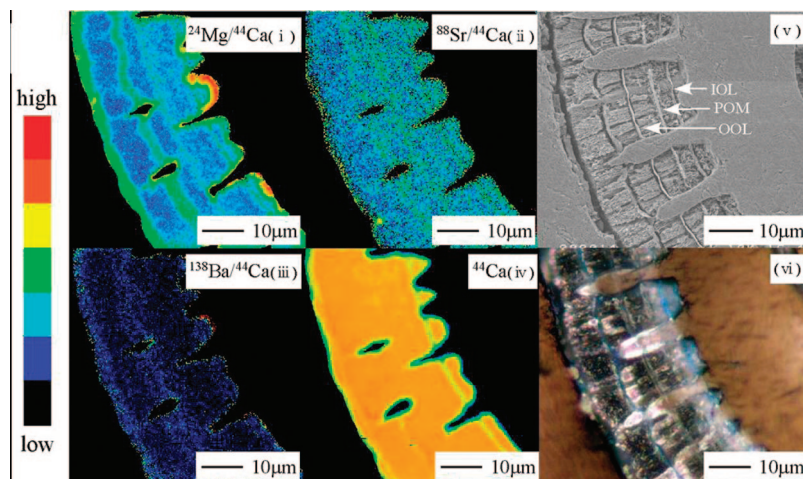
Figure 10. Element distribution and test microstructure of the foraminiferan, *Pulleniatina obliquiloculata*. Distribution of ^{24}Mg/^{44}Ca (g), ^{88}Sr/^{44}Ca (h), ^{138}Ba/^{44}Ca (i), and ^{44}Ca ions (j). Red indicates high concentrations and blue indicates low concentrations. SEM image of sample etched in weak acid with edge-resistant layers indicating organic layers. Reflected light image of (k) stained to reveal protein-rich regions in blue. Ten μm scale bars throughout. Reprinted with permission from ref 119. Copyright 2006 American Geophysical Union.
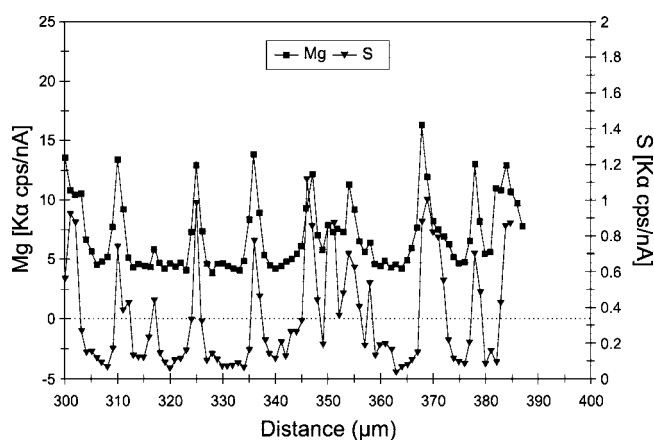
Figure 11. Distribution of Mg and S in test of the perforate foraminifera *Amphistegina lobifera* as determined by electron probe microanalysis (EPMA). Reprinted with permission from ref 106. Copyright 2003 Mineralogical Society of America.

which contains a 12 amino acid sequence homologous to that found in other invertebrate calcium-binding proteins.[136] Perhaps this lack of obvious protein investment in shell formation by such a compact organism is not surprising since the energy-expensive manufacture of proteins to be utilized in biomineralization would have a detrimental effect on DNA synthesis and, hence, physiologically essential proteins. Hence, proteins associated with coccolith formation would be controlling polysaccharide production rather than having a direct involvement in biomineralization.[137] Ozaki et al.[138] isolated what they call an anticalcification polysaccharide from *P. carterae* that may act as an inhibitor to calcium carbonate crystallization.

5.2. Coccoliths—Minor Elements and Stable Isotopes

The micron dimensions of coccoliths inevitably means that trace and minor elements are not measured in a structural context, but rather, analyses are carried out on individual microfossils[139] or from numerous whole organisms. Concerns that coccolith stable isotopes may not reflect those of ambient seawater,[140] being influenced by vital effects, have been allayed by a comprehensive study of eight coccolithophore species in which it was demonstrated that both carbon and

oxygen fractionation are species-specific and correlate inversely with cell size rather than growth or calcification rate.[141] Thus, the unvarying species-specific offset renders the stable isotope composition, a reliable source of paleoenvironmental data.[141] The limitation that cell size imposes on the rate of CO_2 diffusion, relative to carbon fixation, is likely to be the ultimate source of the coccolith stable isotope vital effect.[141]

The fact that modern coccolithophorids occur where supersaturation with respect to calcium carbonate is greatest indicates the importance of the role of seawater chemistry in coccolith production.[142] In vitro studies demonstrate that calcium concentration has a major influence on the structure and rate of deposition of coccolith calcite[143] (Figure 12). Magnesium concentration also has a profound effect on coccolith formation, with high and low magnesium concentrations resulting in malformed coccoliths while flawless coccolith production occurs when the magnesium concentration is that of modern seawater (58 mM)[143] (Figure 13).

While the Sr/Ca ratio of seawater varies by less than 2% globally,[144] field studies reveal that much larger variations in Sr/Ca ratios (~20%) occur in coccolith calcite.[145] Cultures of several species of coccolithophorids reveal a 1−2% increase in Sr/Ca ratio per °C.[146] This result cannot be solely due to temperature since, in an in vitro study comparing five species of coccolithophorids in identical temperature and media conditions, the range of strontium concentration was >30% and was correlated with the rate of calcite production.[144] It is, therefore, necessary to separate the influence of growth rate from that of temperature on coccolith Sr/Ca ratios, and this can be achieved by comparing large species that grow at a rapid rate with small species that grow at a slower rate.[144] It is, therefore, possible to use coccolith strontium concentration to determine past coccolithophorid productivity.[144] Combining Sr/Ca ratios with the carbon isotope fractionation of coccolithophorid alkenones exploits the relationship between the carbon isotopes of organic carbon and the carbon concentration of dissolved CO_2 in seawater and may improve estimates of palaeo-CO_2 levels.[147] Sr/Ca ratio of coccoliths in the Pleistocene is indicative of coccolithophore bloom production.[148] An example of coccolith Sr/Ca ratio reflecting events on the global scale is the increase in oceanic productivity indicated by the marked
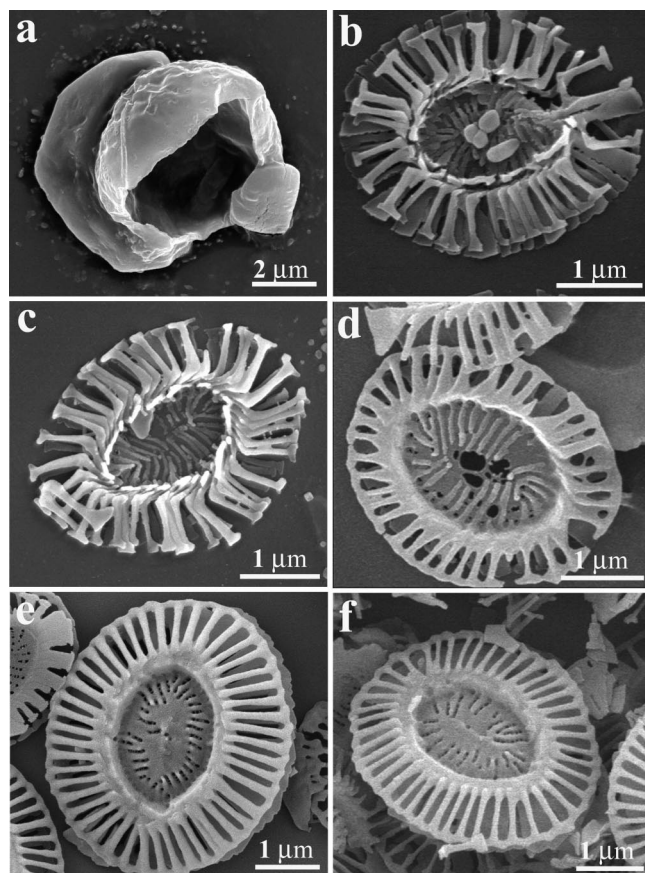
Figure 12. Influence of calcium concentration on coccolith structure in *Emiliania huxleyi*. Cells were grown in artificial seawater containing (a) 0, (b) 1, (c) 2, (d) 4, (e) 10, and (f) 20 mM $CaCl_2$. Scale bar = 1 μm throughout. Reprinted with permission from ref 143. Copyright 2004 Elsevier B.V.

increase in the coccolith Sr/Ca ratio corresponding to the suspected methane hydrate release at the end of the Paleocene, the Paleocene Eocene thermal maximum (PETM).[149,150]

6. Brachiopods

Brachiopods are simple benthic marine organisms with a bivalved shell. The phylum Brachiopoda first appeared in the Cambrian, and there are living brachiopods in all of the world's oceans. The three subphyla[151] are mainly defined via shell mineralogy, with the Linguliformea having shells of francolite, which is a carbonated apatite;[152] the Craniiformea having shells of high Mg-calcite; and the Rhynchonelliformea having shells of low Mg-calcite. The stability of low Mg-calcite and the extensive fossil record makes rhynconelliform brachiopods attractive sources of environmental information.

6.1. Brachiopods—Organic Composition

Investigations into the organic matrix of the phylum Brachiopoda lags far behind that of Mollusca. There are several reasons for this: principally, modern brachiopods are much less abundant and more difficult to obtain, while the ubiquity of molluscs and ease of collection gives them a distinct advantage. As seen from the section on Bivalvia, almost all the proteins that have been sequenced have taken advantage of current molecular biology techniques; to date, a similar approach has not been undertaken for Brachiopoda.
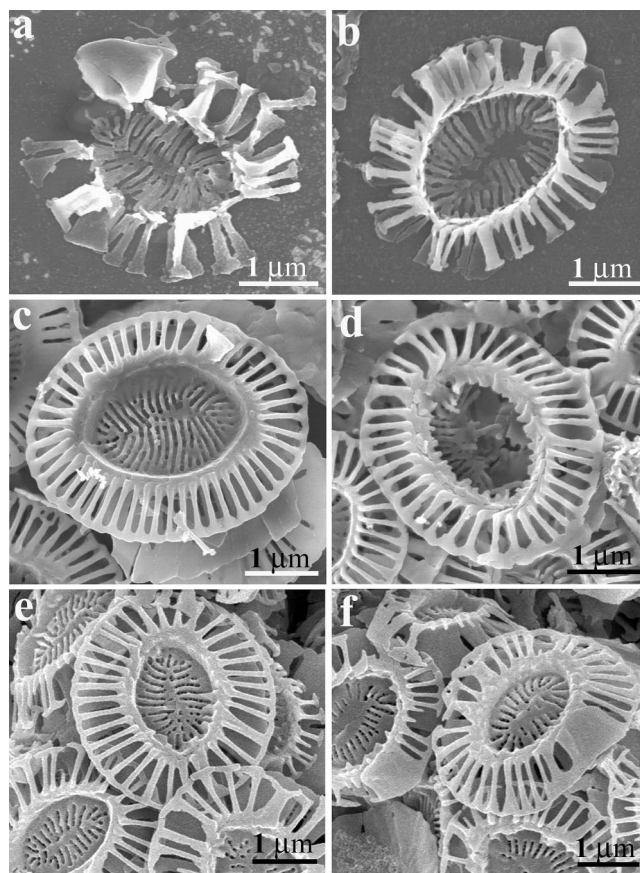
Figure 13. Influence of magnesium concentration on coccolith structure in *Emiliania huxleyi*. Cells were grown in artificial seawater containing (a) 116, (b) 87, (c) 58 (natural level), (d) 29, (e) 15, and (f) 0 mM $MgCl_2$. Scale bar = 1 μm throughout. Reprinted with permission from ref 143. Copyright 2004 Elsevier B.V.

The commercial interest in bivalves associated with the pearl industry also gives a bias toward studying proteins associated with nacre.

Despite this molluscan bias, there is still substantial information on organic material obtained from each of the three brachiopod subphyla: Linguliformea, Craniiformea, and Rhynchonelliformea. Indeed, a substantial amount of work, collating amino acid composition within the shell of invertebrates, was carried out on Brachiopoda by Jope.[153-158]

6.1.1. Linguliformea

Linguliformea are organophosphatic, consisting of carbonate substituted fluorapatite ($Ca_{10}(PO_4)_6F_2$, francolite, FAP) and lacking a hinge mechanism. While calcite-shelled brachiopods contain relatively low levels of organic material (1–5%), the phosphatic-shelled brachiopods contain 25–52% organic material.[153] Although it is apatite crystals rather than calcite or aragonite as in molluscs that are formed and carefully orientated in the shell matrix, it would appear that a very similar mechanism exists whereby a chitin substrate is prepared and cross-linked with glycosaminoglycans and proteins to form a cocoon for crystallization of the apatite granules. The soluble matrix proteins from *Lingula anatina* are perhaps the best characterized for this subphylum.[159,160] Protein fractionation depended on the method used to isolate the proteins from the powdered shell. In the guanadine HCl extract, proteins with an estimated mass from SDS-PAGE of 6, 8.5, 15.5, 21.5, 24, and 44 kDa were observed.

However, with EDTA extracts, additional proteins of molecular mass 4.5, 28, 35, 40, 50, 57.5, 60, and 69 kDa were recorded. The 21.5 and 24 kDa proteins are glycosylated.[160]

In vitro experiments using mixtures of these isolated proteins revealed that they specifically promote crystallization of FAP. Interestingly, the regions from where the proteins were extracted had a clear effect on the kinetics of crystallization with increased crystallogenesis occurring with proteins extracted from the more mineralized region of the shell.[160]

There is a relative dearth of research into the organic matrix of the discinoid brachiopod shell. Williams et al.[161,162] extracted several proteins from the species *Discinisca tenuis*, which gave a number of proteins on SDS-PAGE with apparent molecular weights of 16, 21, 34, 48, 72, and 100 kDa, with a further two more low molecular weight proteins of 13 and 6.5 kDa revealed using silver staining. In this paper, the total amino acid composition of the shells of six living discinid and lingulid brachiopods was also compared, and it showed that, although lingulid shells had a higher organic content relative to discinids, this was not reflected in the amino acid content. Lingulids also had a higher acidic amino acid content.

6.1.2. Craniiformea

The inarticulated brachiopod *Novocrania anomala* is the only species in this subphylum to have its organic matrix analyzed from a living brachiopod,[163−165] although in ref 165, the proteins extracted from several craniiformean fossil shells were compared to the living specimen. *N. anomala* shows two acidic protein bands from SDS-PAGE at 40 and 60 kDa—both are likely to be calcium-binding proteins. By comparing dorsal and ventral valves, it was shown that they differ in their amino acid composition as well as morphology and ultrastructure. From growth experiments on the calcitic shell[163] of *N. anomala*, it was shown that the acidic 40 kDa protein is associated with the interlaminar organic sheets, subsequently determined as chitin, analogous to the chitin−silk fibroin matrix in the aragonite nacre of the Bivalvia (see section on Bivalves), while the glycosylated 60 kDa protein was exclusively intralaminar.

Cusack et al.[164] compared the proteins extracted from two different subphyla *Terebratulina retusa* (Rhynchonelliformea) and *N. anomala* (Craniiformea). The EDTA soluble fractions from *T. retusa* provided proteins of approximate molecular weights 16, 25, 40, 62, and 78 kDa. The amino acid composition of the 40 and 60 kDa proteins from *N. anomala* were compared to the 40 and 62 kDa proteins from *T. retusa*. Although the amino acid compositions are different, they share the same high concentration of acidic amino acids, a low concentration of basic amino acids, and a high glycine content and are likely to be calcium-binding proteins similar to those found in the calcite domains of Mollusca.

6.1.3. Rhynchonelliformea

Earlier studies on intracrystalline proteins extracted from the New Zealand brachiopod *Neothyris lenticularis* isolated three main proteins on SDS-PAGE at apparent molecular weights 47, 16, and 6.5 kDa. Of particular interest is the small 6.5 kDa protein that was later confirmed as a chromoprotein.[166] In this later study, three different living genera, *N. lenticularis*, *Waltonia inconspicua*, and *Terebratella sanguinea*, had a 6.5 kDa protein N-terminal sequenced.
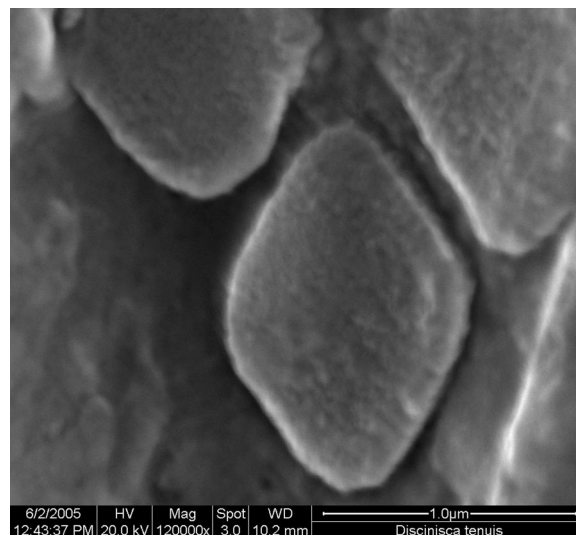
Figure 14. Siliceous tablets on the larval surface of *Discinisca tenuis*. Secondary electron image of siliceous tablets on untreated surface of phosphatic-shelled brachiopod, *Discinisca tenuis*. The siliceous tablets form a regular mosaic. Scale bar = 1 μm.

All three showed homology, and IR spectroscopy confirmed that the coloration was due to the presence of carotenoid molecules associated with the protein.

In an attempt to define which proteins were located in specific areas of the brachiopod shell structure, Cusack et al.[167] used shells from three extant rhynchonelliform orders. The thecidienes, *Thecidellina blochmanni* and *Lacazella mediterranea*, consist almost exclusively of primary layer; *Notosaria nigricans* and *T. retusa* are composed of primary and secondary layers; while *Liothyrella neozelamica* and *Liothyrella uva antartica* include a tertiary layer as well as primary and secondary shell successions. Although the study detected proteins in the range 20−107 kDa with some shells providing more proteins than others, there was no evidence of proteins being specific to a particular layer, even though several proteins were common to more than one species.

A more recent review of shell-soluble proteins from Rhynchonelliformea[168] alludes to the similarity between the monocrystals, or granules,[167] that make up the fibrous calcitic layers and calcite prism formation the pteriomorphid bivalves. In this review, the shell organic matrix was extracted from five genera. Different staining techniques highlighted different proteins over a very broad spectrum of molecular weights. This draws attention to the importance and care needed if soluble shell proteins are to be identified using SDS-PAGE. The effect of adding the proteins isolated from individual genera was tested on $CaCO_3$ precipitation experiments, and although it produced spectacular results in changes in crystal morphologies, the effect was not identical from species to species.

6.2. Brachiopods—Minor Element Composition

Linguliform brachiopods are unusual, but not unique,[169] among invertebrates in having shells of calcium phosphate[161,170−174] in the form of francolite, which is a carbonate-containing calcium fluorapatite.[172] The degree of orientation of apatite correlates with that of β-chitin.[175,176] Linguliform shells have a high organic content.[177] The larval surface of the apatite shells of discinid brachiopods is covered in siliceous tablets (Figure 14)[165,178] that are preformed in vesicles and then extruded[179] (Figure 15). This is analogous to the mechanism
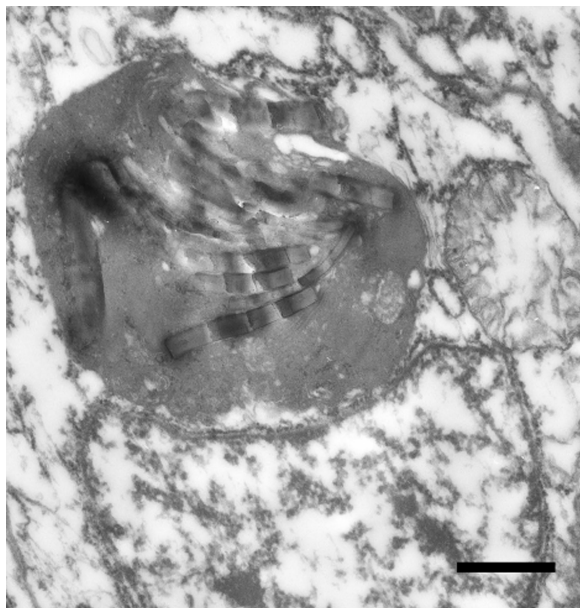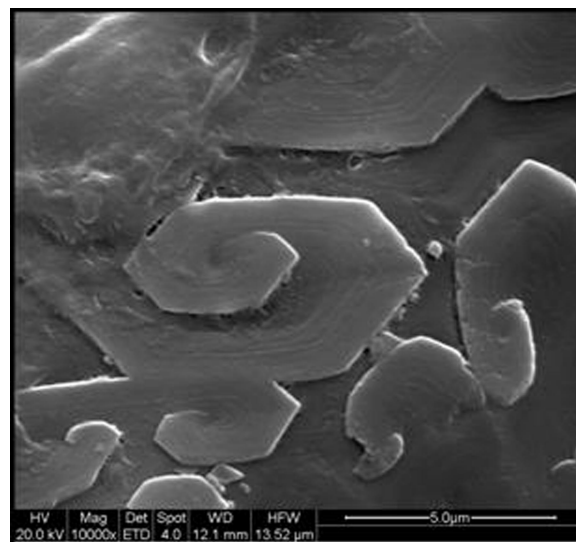
Figure 15. Siliceous tablets of *Discinisca tenuis* within intracellular vesicle. Transmission electron micrograph of siliceous tablets in intracellular vesicle of *D. tenuis*. Scale bar = 1 μm. Reprinted with permission from ref 179. Copyright 2004 Royal Society of London.

Figure 16. Calcite semi-nacre in *Novocrania anomala*. Secondary electron image of calcite semi-nacre in the shell of the Craniid brachiopod, *Novocrania anomala*. Scale bar = 5 μm. Reprinted with permission from ref 184. Copyright 2007 Blackwell Publishing.

Figure 17. Crystallographic orientation of calcite semi-nacre in *Novocrania anomala* shell as determined using electron backscatter diffraction (EBSD). Crystallographic orientation of calcite semi-nacre laminae indicated using color key. Shell exterior toward top of image. Wire frames demonstrate that, while overall, the calcite *c*-axis is parallel with the shell exterior, it follows the undulations of the laminae. Scale bar = 30 μm.
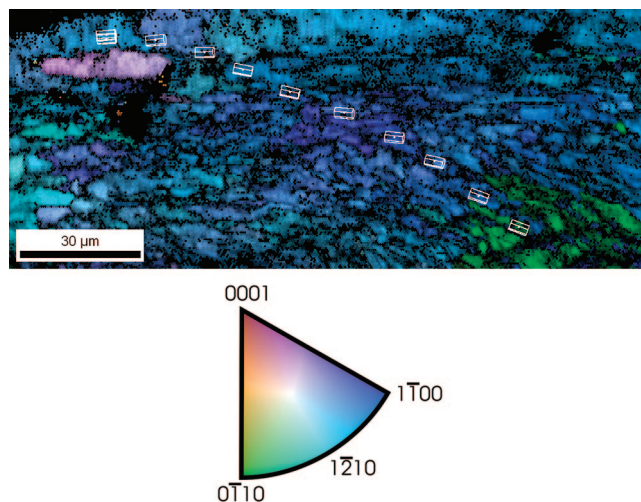
employed by coccolithophorids where the elaborate calcite plates are manufactured in intracellular vesicles and then transported to the cell surface.[180] Switching from silica to phosphate production is likely to represent a significant change in secretory regime. The function of these siliceous tablets or why the biomineral production should switch in this way is unknown but begs fundamental questions about the regulation of such a dramatic switch in secretory regime. It has been suggested that at least some of the imprints on acrotretide brachiopods were formed by calcite tablets.[181] This suggestion and the discovery of calcite granules within phosphatic shelled brachiopods from the early Cambrian[182] all pose intriguing questions about the evolution and selection of different mineral systems in biology as well as within the phylum Brachiopoda.

Craniid brachiopods have a high Mg concentration[153,177] that is consistent through the primary and secondary layer of the shell.[183,184] The secondary layer has been described as semi-nacre[185] according to the terminology established for bryozoans[186] to describe calcite that grows by screw dislocation and resembles the structure of aragonite nacre (Figure 16). The *c*-axis of craniid semi-nacre is more or less parallel to the shell exterior, undulating with the laminae[185] (Figure 17). In *Novocrania anomala*, Mg and S concentrations are both constant throughout the shell thickness.[184]

Rhynchonelliform brachiopods are characterized by an outer (primary) layer of fine-grained calcite underlain by the secondary layer of calcite fibers (Figure 1D). The calcite fibers comprising the secondary layer of low Mg-calcite brachiopods are composed of granules that are added incrementally as the fiber grows.[168] The fibers are parallel with the shell surface, yet the *c*-axis is perpendicular to the shell surface[187,188] (Figure 18). Biology, therefore, controls the crystallographic orientation of the component granules. Similar patterns occur in the distribution of elements such as magnesium and strontium, which are present in higher concentrations in the primary layer and decrease toward the shell interior. The trace element distribution is not constant

in rhynchonelliform brachiopods with higher concentrations of Mg, S, and Sr in the primary layer and the outer part of the secondary layer.[185] Strontium and magnesium reach fairly constant concentrations in the inner part of the shell, with the concentration of magnesium relating to water temperature.[189]

6.3. Brachiopods—Stable Isotope Composition

In 1961, Lowenstam[35] pioneered the work on brachiopod shell stable isotopes by demonstrating that the low-Mg calcite of the Rhynchonelliformea is in oxygen isotope equilibrium with the seawater. There then followed very many studies of past climate change using brachiopod oxygen isotope composition.[190−192] While the (inner) secondary layer of low Mg-calcite shelled brachiopods is in oxygen isotope equilibrium with ambient seawater, the (outer) primary layer is
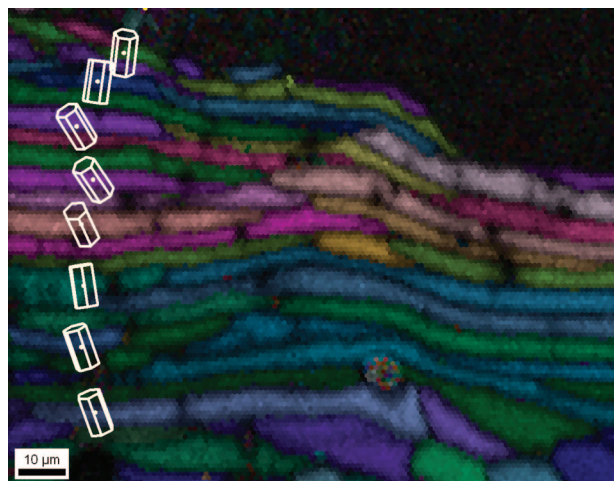
Figure 18. Crystallographic orientation of calcite fibers in *Terebratulina retusa* shell as determined using electron backscatter diffraction (EBSD). Crystallographic orientation map of calcite of the secondary layer fibers in *T. retusa* (cf Figure 1D) according to color key in Figure 17. The dark region toward the top is the primary layer. Wire frames indicate that the *c*-axis of calcite is perpendicular to the fiber axis and to the shell exterior. Scale bar = 10 μm.
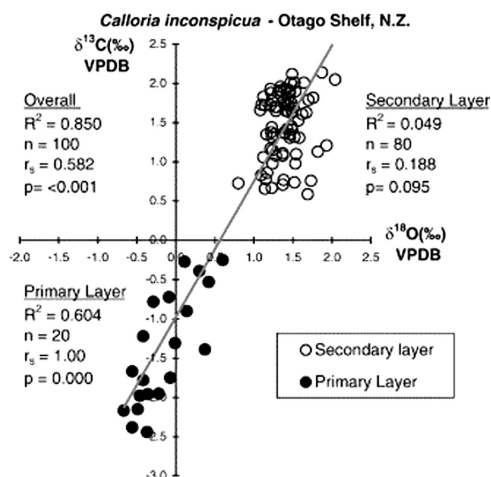
Figure 19. Cross-plot of stable isotope composition (δ^{18}O and δ^{13}C) of primary and secondary layer of calcite of *Calloria inconspicua* shell. Reprinted with permission from ref 13. Copyright 2005 Elsevier B.V.

isotopically lighter for both carbon and oxygen[13,14] (Figure 19). The covariance of oxygen and carbon isotopes suggests a kinetic effect resulting in the isotopically light primary layer. In the secondary layer, there is a decoupling of the carbon and oxygen isotope composition. The oxygen isotope composition is fairly constant, even in specialized structures such as the loop or pedicle foramen, while the carbon isotope composition shows a fairly consistent relationship with structure, suggesting some physiological prioritization[13] (Figure 20). Despite all of the biological control evident in morphology and crystallography (Figure 1D and Figure 18), the secondary layer calcite is in oxygen isotope equilibrium with ambient seawater. The fact that the secondary layer calcite fibers of rhynchonelliform brachiopods are in oxygen isotope equilibrium with ambient seawater is counterintuitive given the concern over the influence of vital effects on the recording of environmental information. Counterintuitive as the relationship may be, it has enabled brachiopods to be used in numerous investigations of palaeoenvironments.[191,193−196] Auclair[197] demonstrated that, in modern

Figure 20. Relative carbon isotope values for the specialized and nonspecialized regions of the secondary layer of dorsal and ventral valves of rhynchonelliform brachiopods. Reprinted with permission from ref 291. Copyright 2004 David Parkinson.
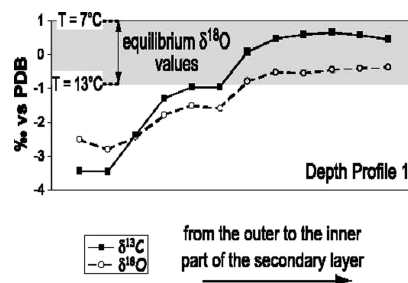
Figure 21. Stable isotope composition throughout the thickness of the secondary layer of the shell of the rhynchonelliform brachiopod *Terebratalia transversa*. [197] Reprinted with permission from ref 197. Copyright 2003 Elsevier B.V.

Terebratalia transversa, oxygen isotope equilibrium is not achieved in the first formed primary layer but rather is reached as fibers are added to the growing shell such that the innermost part of mature brachiopods is in oxygen isotope equilibrium with the seawater (Figure 21). This observation is important since, if the observations in *T. transversa* apply to all rhynchonelliform brachiopods, then the implication is that it is not simply the innermost secondary layer calcite that is in oxygen isotope equilibrium with ambient seawater but the innermost secondary calcite of mature valves. Even in linguliform brachiopods with shells composed of carbonate-containing calcium fluorapatite, the oxygen isotope composition of the carbonate component can be used as a seawater temperature proxy.[198]

7. Molluscs

This huge phylum contains a vast array of biomineral structures. To limit this review, we focus on bivalve molluscs, since their accomplishments in biomineralization raise some of the key questions in the field. Much research interest is focused on bimineralic molluscs (Figure 22A), partly because of the occurrence of aragonite nacre, which has attractive material properties, being tough and strong, yet light.[199,200] Also of interest is that, in many bivalve shells, nacre is accompanied by a prismatic layer (Figures 22B and 25A). Indeed, it has been suggested that nacre evolved from the aragonite prismatic layer.[201] These bitextured shells are often bimineralic, since the prisms can be composed of calcite, such as in *Mytilus edulis*, or aragonite, as in *Modiolus modiolus*, for example. In bivalve molluscs, the switch during shell growth from calcite, the low-pressure polymorph of calcium carbonate, to aragonite, which is the high-pressure metastable polymorph, appears routine. Indeed, bitextured and often bimineralic shells are almost the trademark of the Bivalvia and will inevitably result in differences in organic and inorganic compositions between the two layers.
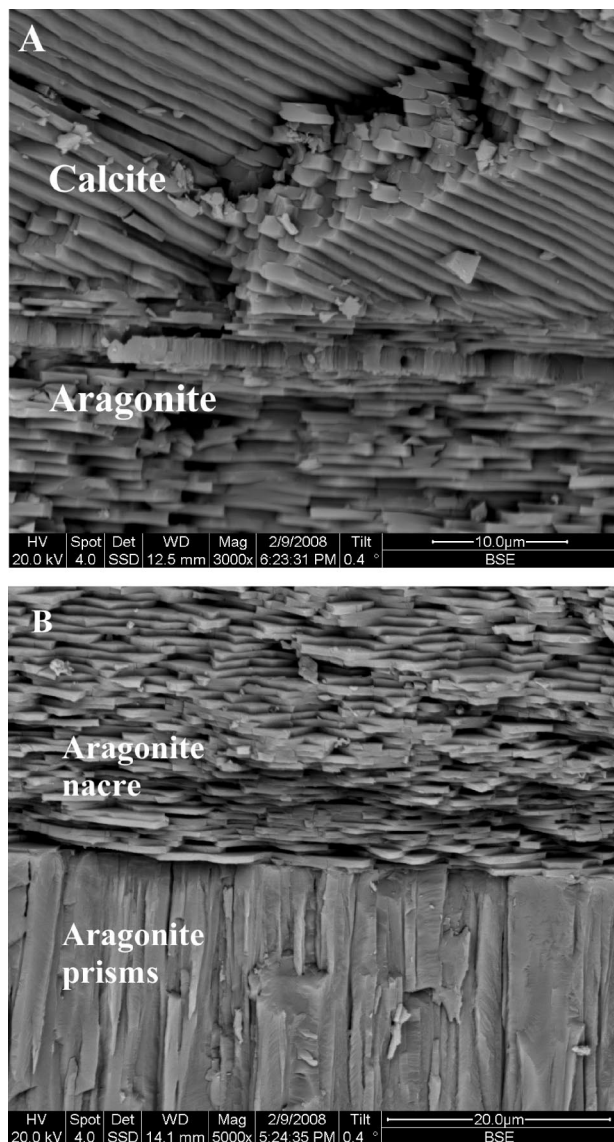
**Figure 22.** Backscattered electron image of fracture section of two bivalves. (A) The bimineralic *Mytilus edulis* with calcite prisms to the exterior (top) and aragonite nacre to the interior (bottom). Scale bar = 10 μm. (B) Interface between aragonite nacre (top) and aragonite prisms (bottom) at the innermost shell of *Modiolus modiolus*. Scale bar = 20 μm.

7.1. Bivalve Molluscs—Organic Composition

The organic matrix of bivalves, and proteins therein, are by far the most studied of all the phyla, leading to a relatively comprehensive, though tentative, understanding of protein involvement in biomineralization. By stringent analysis of proteins bound in specific areas of shell, researchers have started to piece together the relationship between several proteins, crystallogenesis, polymorph outcome, and growth inhibition.

For an excellent and comprehensive review of molluscan shell proteins encompassing a broad perspective, readers are directed to the review by Marin et al.,[202] where the 44 molluscan proteins are grouped according to pI values. An equally good review covering all 77 invertebrate skeletal proteins and including a comment on the osteogenic properties of nacre can be found in the manuscript by Sarashina and Endo.[203] A complementary review by Zhang and Zhang[204] highlights the proteins as to location either in nacreous or calcitic layer. A useful list of illustrated
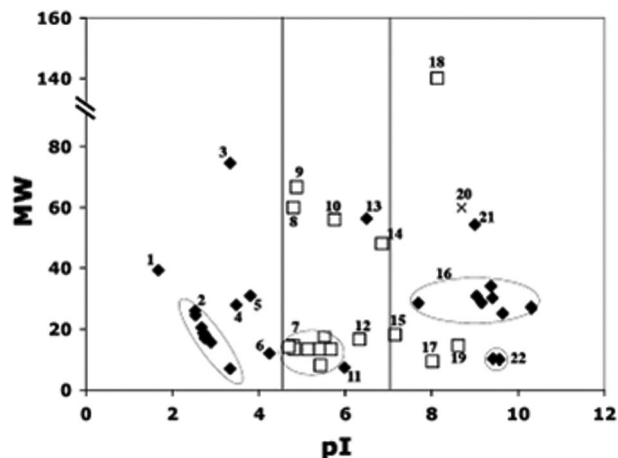
Figure 23. Molluscan shell proteins according to their molecular weight and pI values. Open squares indicate those proteins associated with aragonite; filled diamonds indicate those associated with calcite; and crosses indicate proteins associated with both polymorphs. 1 = aspein; 2 = Asp-rich proteins; 3 = MSP-1; 4 = MSP-2; 5 = MS131; 6 = prismalin-14; 7 = N-14/N16/pearlin/ perline proteins masking AP7 and AP24; 8 = MS160; 9 = mucoperlin; 10 = nacrein from *P. fucata*; 11 = MSI7; 12 = dermatopontin; 13 = tyrosinase-like1; 14 = nacrein from *T. marmoratus*; 15 = perlucin; 16 = shematrin proteins; 17 = perlustrin; 18 = lustrin A; 19 = perlwapin; 20 = N-66; 21 = tyrosine-like2; 22 = KRMPs. Reprinted with permission from ref 202. Copyright 2008 Elsevier B.V.

molluscan shell morphologies, and their location in the shell matrix, can be found in the manuscript by Kobayashi and Samata.[205]

Here, the salient features of these recent reviews and some additional material are presented. The fascination lies in gaining an understanding of how the shell building material is recruited, probably from the extrapallial pocket/fluid, and sacrificed on a carefully constructed template in a highly and precisely controlled manner.

Although proteinaceous material is present in relatively small amounts (between 0.03 and 0.5 wt % in the soluble fraction), great endeavors have been made over the past few decades to isolate proteins from within specific areas of the shell matrix and characterize them at least to the primary amino acid level. Indeed, it is a tribute to the tenacity of many researchers that so many proteins have now been characterized. As with several areas of biomineralization, significant progress had to wait for major advances in technology to achieve success; on the protein front, advances in molecular biology through RT-PCR or cDNA library oligoscreening provided an access route to proteins that were near unobtainable in the native form. Indeed, most of the molluscan proteins described in this section have been obtained from cDNA expression libraries.

Marin characterizes the molluscan shell proteins into three groups, according to their theoretical isoelectric point, pI. This is a useful approach to infer approximate classification and almost serendipitously defines the location of the protein within the shell architecture. Figure 23 shows a graphical representation of the distribution of molecular weights versus pI values. The three groups are as follows: extremely acidic with a pI below 4.5; moderately acidic with pI between 4.5 and 7; and basic shell proteins with a pI greater than 7.

The most acidic proteins are the most homogeneous group and are exclusively associated with calcitic shell layers. There are two strong, identifiable characteristics of the six mol-

luscan proteins characterized so far—almost all are Aspartic acid (Asp) rich and most have several short, repeated sequences. Among the 77 invertebrate skeletal proteins surveyed by Sarashina and Endo,[203] 43 were acidic (pI < 6.0), 20 were neutral, and 14 were basic (pI > 8.0). Of these, the most acidic are Aspein, pI = 1.5, with 60% Asp;[77] the Asp-rich family, pI = 2.5, 45% Asp;[206] and MSP-1, pI = 3.2, Asp 20%.[207,208] As a consequence, the preponderance of Asp residues in these proteins characterizes them as low-affinity, high-capacity calcium-binding proteins.[209] Aspein and Asp-rich are probably homologous proteins sharing 48% sequence similarity, while MSP-2 shows 91% identity with MSP-1 and is likely to be a truncated form of the latter.

MSI31, a Gly-rich protein from the insoluble matrix,[210] is expressed only on the edge of the mantle[210,211] and is deemed important in the formation of the calcitic prismatic layer framework. The 10 polygly rich domains are thought to participate in the formation of β-sheet structures that may be a prerequisite in laying down the prismatic layer. Prismalin-14, another protein belonging to the mantle edge, is a Gly/Tyr rich protein from the insoluble hydrophobic framework of the prismatic layer,[212] appears to inhibit $CaCO_3$ precipitation, and induces changes in the morphology of calcite crystals.

A common feature across all invertebrate phyla is the ubiquity of sequence repeats, and it is no less so for these extremely acidic proteins—in fact, it appears essential to their function. Briefly, these repeats range from a 58 poly-Asp block of 2–10 units, where $(Asp)_3$ is the most common with 27 repeats, found in Aspein to a variable acidic domain in the Asp-rich family containing long poly-Asp stretches coupled with DEAD repeats. Aspein has a high sequence identity to Aspolin,[211] which is a highly acidic Asp-rich protein from fish muscle. Interestingly, Aspein, which directs calcite formation, also shows sequence similarities to fibrogen-binding and bone sialo-binding proteins.

The Asp-rich family of seven homologous proteins are thought to be the product of alternate splicing of the same gene. The acidic domain shows similar sequence similarity (up to 68%) to Calsequestrin,[213] a calcium-binding protein from cardiac and skeletal muscle that has been shown to interact with calcium ions on its surface. The presence of the DEAD repeats is thought to be involved with Mg^{2+} acquisition, though, at present, it is unclear why.

MSP-1, a major water-soluble glycoprotein from the scallop *Patinopecten yessoensis*, is a little more unusual from Aspein and the Asp-rich proteins in having a more modular-based structure focused in the central region of the protein comprising a highly conserved unit of between 158–177 amino acids repeated 4 times in tandem. The overall domain arrangements in MSP-1 are very similar to those seen in Lustrin A (below) and, in particular, a stretch of 29–43 residues dominated by serine and glycine (SG) repeats. In both MSP-1 and Lustrin A, these SG domains confer a high degree of flexibility and are seen as linkers or spacers between the D and K domains.

More recently, a soluble 18 kDa Asp-rich protein (pI = 3.9) has been isolated from the myostracum of the oyster shell *Crassostrea gigas*.[214] CD analysis shows the putative calcium-binding Asp domains located in the α-helix and turn domains rather than in the β-structure.

The second group, containing moderately acidic proteins (pI between 4.5 and 7), forms a rather disparate collection of proteins. The first, and most studied, in this group is
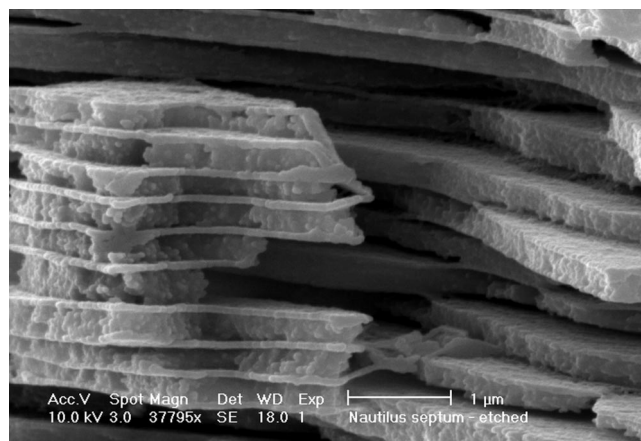
Figure 24. Scanning electron microscope (SEM) images of fracture section of *Nautilus* nacre, after slight etching with EDTA, fixation, and critical-point drying (CPD). Scale bar = 1 μm. Reprinted with permission from ref 225. Copyright 2006 Wiley-VCH Verlag GmbH & Co. KGaA.

nacrein,[215] which appears to have a diversity of subdomain function ranging from calcium-binding activity through a total of 26 tandem repeats of G-X-N, where X is usually D, N, or E, to carbonic anhydrase activity consistent with three zinc-binding histidine residues.

Further studies[216,217] showed that nacrein could be retrieved from both the prismatic and nacreous layer. A homologous protein, N66, isolated from several different species, displays two carbonic anhydrase subdomains as well as longer repeat domains comprising 46 G-X-N motifs interspersed with G-N repeats and, consequently, infers a more basic pI and, hence, is less likely to show calcium-binding activity.

Among the more interesting proteins retrieved from the nacreous layer of *P. fucata* is the insoluble framework protein MSI60[210] specific to the nacreous layer.[211] MSI60 appears to have a number of domains that indicate a diverse function. Eleven polyalanine blocks of between 9 and 13 residues is similar to spider silk fibroin, and 39 polyglycine blocks of 3–15 residues is consistent with β-sheet formation. Combining these features with two Asp-rich domains suggests sufficient organization to implant calcium ions in a regulated manner and also, via cysteine residues, to form intermolecular disulfide bonds with other macromolecules in the nacreous layer.

Within this section, there are also the low molecular weight proteins N14/N16[217−219] otherwise called pearlin.[220,221] Both are specific to the nacre layer with the expression of N16 correlated to that of nacrein.[211] Both proteins inhibit calcium carbonate precipitation in solution and induce platy aragonitic tablets when absorbed on insoluble matrix membranes.[217,218]

Recently, a novel 19 kDa protein named N19 was extracted from the water-insoluble fraction of the nacreous layer of *P. fucata*.[222] N19 has been found to have an inhibitory effect on calcium carbonate crystallization. Furthermore, Northern blot studies of total RNA from the mantle pallial edge showed the N19 transcript to be more abundant in the pallial region of the mantle, suggesting the protein is expressed in the pallial region and then translocated into the nacreous layer, where it has a negative effect on nacreous layer formation.

The heavily glycosylated mucoperlin from the bivalve *Pinna nobilis*[223,224] has been affiliated to the mucin family to which it attributes epithelial lubrication and gel-forming
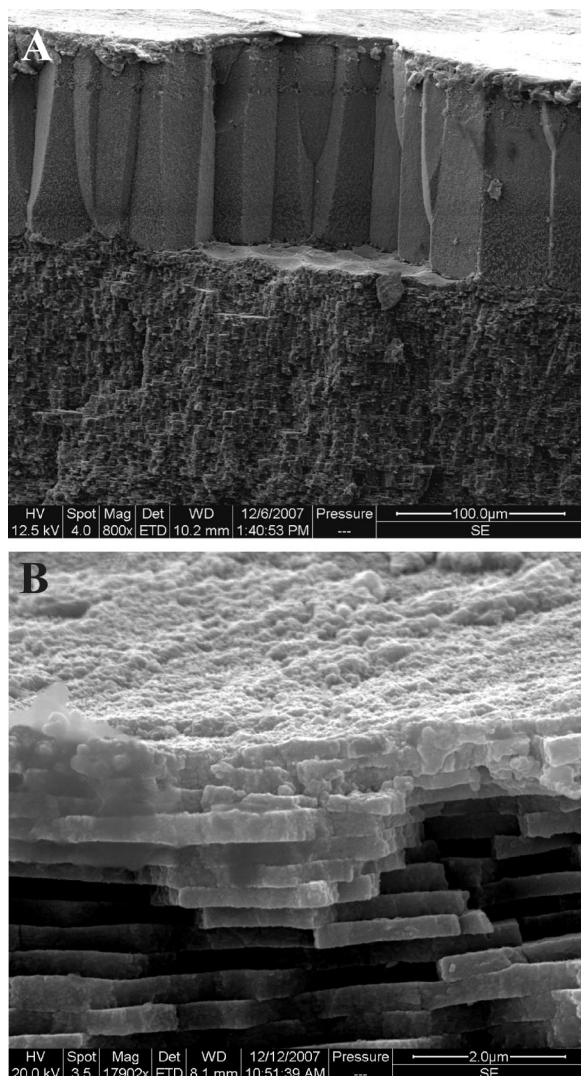
Figure 25. Aragonite prisms and nacre in the freshwater bivalve, *Anodonta cygnea*. (A) Secondary electron image of a gold-coated fracture section of *A. cygnea* showing the interface between the outer prisms and inner nacreous layer. Scale bar =100 μm. (B) Close up of prism–nacre interface revealing organic material and the nature of the interface. Scale bar = 2 μm. Images from Peter Chung and Daniel Greenwood (University of Glasgow).

abilities. Found only in the nacreous layer, the 66.7 kDa protein is concentrated around the tablets, particularly on the lateral sides, and may be a component of a gel-like matrix (Figure 24) that is pushed apart during nacre tablet growth.[225] Marin et al.[223] also observed that this snug fit of mucoperlin around the tablets may function in a mechanism similar to that described by Wheeler et al.,[227] which terminates crystal growth. Addadi et al.[225] take a refreshing look at the individual components involved in forming the nacre structure. They do this within the context of current biochemical knowledge about the proteins and propose a stepwise procedure that possibly involves a silk-like protein with water playing a crucial role in controlling its structure.[228]

Simultaneously, with the isolation of mucoperlin, two other proteins have been isolated from *P. nobilis*.[229] Both are associated with the calcitic prismatic layer. Caspartin is a 17 kDa Asp-rich protein that was shown to strongly interact with growing CaCO$_3$ crystals, inducing changes in shape and increased size. The second protein, named calprismin, 38 kDa, is less acidic than caspartin and, at present, has no defined function.

Two abalone *Holiotis rufescens* water-soluble proteins AP7 and AP24[230,231] containing two putative calcium-binding domains were isolated from the soluble matrix of the nacreous layer. Studies of a synthetic 30 amino acid N-termini of AP7[232] and both AP7 and AP24[233] by NMR and CD showed random coil-like structures. Both proteins may inhibit calcite growth in vitro, by binding directly to the calcite step edges via their N-termini. From the same species of abalone, another acidic Asp-Gly rich protein named AP8 has been isolated from the ammonium sulfate supernatant obtained from the soluble nacre protein fraction.[234] AP8 appears to exist as two isoforms: AP8-α (8.7 kDa) and AP8-β (7.8 kDa). In vitro crystal growth of calcite on a Kevlar substrate to which AP8, AP7, and AP24 had been added determined that only the AP8 proteins had the ability to modify calcite morphology.

A little out of place in this group with a predicted pI of 5.98 is MSI7 isolated from the Japanese oyster *Pinctada fucata*.[235] MSI7 shows high sequence similarity to the N-terminal half of the acidic protein MSI31 and may be a truncated form of the latter. Both MSI31 and MSI7 contain the same polyglycine blocks. Since the transcript of MSI31 is only expressed on the cusp of the mantle (calcitic prisms)[210,211] and MSI7 is expressed in both the nacreous dorsal and the prismatic mantle edge, then MSI7 could be thought of as a transition protein.

The final group of molluscan shell proteins is dominated by the multifunctional basic protein Lustrin A.[236] Rich in serine, proline, and glycine, it is the largest protein to be sequenced in this phyla (1428 amino acids in total). Extracted from the nacreous layer of the abalone *H. rufescens*, this modular structure has been the subject of several studies to try and elucidate structure–function relationships.[237–241]

Perlustrin,[242,243] perlucin,[242,244] perlwapin,[245] and perlinhibin[246] are four proteins isolated from the nacreous layer of the abalone *H. laevigata*.

Perlustrin presents 40% similarity to mammalian insulin growth factor-binding protein (IGF-BP) through the N-terminal domain.[243] Experimentally, perlustrin binds both human insulin type growth factors (IGFs) and bovine insulin, which gives credence to the hypothesis that phylogenetically biomineralization systems such as nacre and bone may contain components inherited from common ancestors.[228,247–250] Perlucin, a 155 amino acid protein containing an N-glycosylated asparagine, displays similarities to the C-type calcium dependent domain of C-type lectins with a divalent metal ion-dependent ability to bind to glycoproteins containing galactose or mannose/glucose.[244] Perlucin enhances the nucleation of calcium carbonate on calcite surfaces and, as a result, is incorporated into the crystal lattice.[251] Perlwapin, which has a high sequence identity with the C-terminus of lustrin A, is so-called because of partial homology to whey acid proteins (WAPs) that are characterized by a conserved pattern of 8 Cys residues, which are involved in disulfide bond formation. Functionally, it inhibits calcium carbonate precipitation by selective binding to distinct step edges preventing further crystal growth.

In vitro studies[246] of perlinhibin show that it inhibits the growth of calcite and induces the formation of nacre. Mann et al.[246] also showed that perlinhibin induces the growth of flat, orientated aragonite crystals.

Several newly identified proteins with a pI above 9 have been identified from *P. fucata*. They are grouped into two families: K-rich matrix proteins (KRMPs) and shematrin.

KRMPs are three small homologous Lys-Gly-Tyr rich proteins.[252] The Lys rich domain, which is 40 amino acids long, comprising all the Cys and Trp residues, may interact with negatively charged ions (bicarbonate) or acidic matrix proteins. Functionally, KRMPs may be linker proteins between acid-soluble proteins and hydrophobic framework proteins of the prisms.

The final group of proteins, the shematrins, comprise seven glycine-rich proteins of molecular weights between 25−33 kDa.[253] Apart from shematrin-5, pI = 7.7, all have pIs in the range 9−10.2. Although the C-terminus of all shematrins have a basic RKKKY, RRKKY, or RRRKY motif, shematrin-2 has a Gly-rich domain analogous to the acidic MSI31 and shematrin-5 contains an acidic domain homologous to the most acidic Aspein (pI = 1.5).

The functionality of many of these proteins has been determined using a chitin−silk and acidic macromolecule assembly, which is a reliable assay for testing either individual proteins or mixtures to induce calcium carbonate deposition or polymorph control and nucleation.[74]

7.2. Mollusc Shell Formation—The Nacre Model

With the increase in knowledge about the possible functions of these proteins, which have been derived directly from specific shell layers, researchers are beginning to piece together a potential mechanism for shell formation. In the past few years, several papers, describing possible mechanisms of nacre formation, appear to be reaching some general consensus on the process of biomineral self-assembly.[223,225,254−259] Consensus favors the initial assembly of an organic womb or cocoon before crystallogenesis takes place. There is, however, possibly less consensus about what is exercising this control in the building process—direct/indirect cellular control or physical and chemical control. Perhaps the dichotomy is derived from the standpoint of where the building materials are recruited—via mantle cells in the form of mineral-loaded vesicles, delivered to the site of mineralization by the cells, or from the extrapallial fluid, where some sort of partial self-assembly is engineered by protein−protein and/or protein−carbohydrate interactions, before being sacrificed on the cellular template. These cellular processes may well be mediated through the extrapallial space. Throughout ontogeny, both events are likely to occur—initially cellular processes dominate and then, once established, a more biophysical approach prevails. It is, however, more likely that the basic building blocks are recruited directly or indirectly from the EP fluid, although at present the definitive link between those proteins derived directly from the shell and those proteins isolated from the EP fluid is still to be made. This may well be due to the present paucity of proteins isolated and characterized directly from the EP fluid. Hattan et al.[260] found that the main EP protein (a dimer of ca. 28 kDa monomers) was highly glycosylated, bound calcium, and, in so doing, formed large self-assemblages of high-order protomers. Further work on this protein by Yin et al.[261] determined it to be multifunctional, serving as a calcium transport protein and a shell matrix protein and also involved in heavy metal detoxification. Perhaps, after all, we are starting to see a link between EP proteins and shell proteins. There will undoubtedly be a greater melange of proteins in the EP fluid since there will be several proteins needed for the signaling process between the shell, the extrapallial compartment, and the animal.

The foundation material in the assemblage is undoubtedly the biopolymer β-chitin,[262] which is excreted by the animal from the mantle into the extrapallial space. Levi-Kalisman et al.[263] showed a self-assembly of chitin biopolymers with crystallites 20−30 nm in diameter and several hundred nanometers long. These chitin crystallites then self-assemble into a mesophase, partially ordered, liquid crystal. Since new nacre layers are laid down every 1−24 h,[264] time constraints disallow a totally ordered liquid crystal structure. By using histochemical techniques, Nudelman et al.[258] have mapped the matrix surface of a single tablet and have shown that the center of the tablet is not only rich in carboxylates and sulfates but also contains aragonite nucleating proteins.

In an analogous manner, Nudelman et al.,[256] using recombinant green fluorescent protein-tagged chitin-binding protein (CBGFP), have shown that chitin is present within calcite prisms in the form of an intracrystalline network of fibers and is not located between prisms. In the same study, using fluorescent antibodies against Asprich proteins, it was also shown that these Asprich proteins were distributed throughout the prism in a pattern similar to that of the chitin-binding protein and were an integral component of the intracrystalline organic matrix. By contrast, the interprismatic matrix, or prism envelope, is composed mainly of Gly rich proteins.

The next process could well involve what is termed prismatic framework proteins—proteins that are rich in Gly, have an affinity for chitin, and are often linked to silk-like proteins or silk fibroin. The interactions of these additional macromolecules stabilizes the chitin crystallites and produces a fibrous membrane conducive to crystal nucleation. Nudelman et al.[256] determined that this major component of the matrix, silk fibroin, is not an integral constituent of the chitin sheets. Pereira-Mouries[259] observed that, in the bivalve *Pinctada maxima*, the silk-like proteins formed a hydrated gel "sandwich"[225] (Figure 24) between chitin layers and, hence, provided a hydrophobic environment conducive to nucleation of aragonite crystals. This concept is further developed to give a more complete understanding of biomineralization.[225] In Figure 25, we see further evidence of this laying down of an organic substrate: this time in what seems like a cement foundation between prisms and tablets. Further SEM studies by Nudelman et al. enhance this observation.[255]

As seen from the brief descriptions of the proteins listed previously, many are multifunctional and are well-equipped to fulfill the protein stabilizing role: e.g., Lustrin A, mucoperlin, nacrein, MSP-1, and MSI60, with acidic calcium-binding domains, glycine rich domains, glycosylation domains, and even domains with positively charged amino acids that may interact with carbonate ions.

The final stage in the process is the nucleation of individual aragonite tablets. Up until now, only the infrastructure for aragonite construction has been accomplished (Figure 26 parts A−D). It is almost certain that, at this stage, the calcium carbonate is present in the amorphous phase (ACC)[40,41,265] and is likely to be transported from somewhere within the mantle encapsulated within a vesicle.[225] Whether this vesicle diffuses across the extrapallial region and attaches to a receptor on the shell side is unclear at present. This arrangement would get around both logistical and energetic requirements. In in vitro, abiotic experiments, $CaCO_3$ will crystallize as calcite, yet many invertebrates will conveniently produce calcium carbonate as the mesostable aragonite polymorph. This control is exerted by the protein environ-
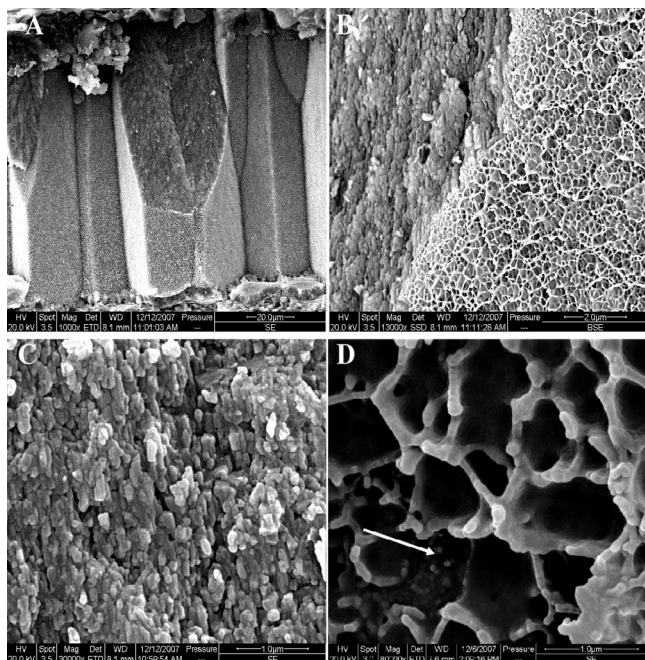
Figure 26. Detail of aragonite prisms in the bivalve *Anodonta cygnea* showing juxtaposition of granules and organic matrix. (A) Broken prism as in Figure 25A. Scale bar = 20 μm. (B) Close up of (A) revealing granular composition of prism (left) with outer organic meshwork (right). Scale bar = 2 μm. (C) Close up of granules in (B). Scale bar = 1 μm. (D) High magnification image of organic meshwork showing granules (arrow) encased within the organic sheath. Scale bar = 1 μm. Images from Peter Chung and Daniel Greenwood (University of Glasgow).

ment, and it has been shown that proteins in the calcite layer will produce calcite and those extracted from the nacreous layer will produce nacre.[74,266] This stage of crystallogenesis may be catalyzed by the acidic calcium-binding proteins that have been adsorbed on the chitin−silk substrate. The actual construction of the nacre brick wall is intriguing, since the spatial arrangement is highly ordered. As mentioned earlier, Nudelman et al.[258] have shown that carboxylates and sulfates were detected at the very center of a nacre tablet, and this may act as a precise locating sensor to begin crystal growth.

These aragonite bricks and aragonite or calcite prisms are made from individual granules (Figure 26). How are they formed in such a precise way in such a regular shape? There are now several good theories on how this biomineral bricklayer sets about the task of interlocking these nacre tablets.[267−271]

7.3. Bivalve Mollusc Minor Elements and Stable Isotopes

Just as specific proteins are associated with the different shell layers, inevitable differences occur in the trace and minor element composition of these layers. Of equal importance are the differences that occur within a shell layer, which, in terms of morphology, appears constant. Detailed information is important here to inform our understanding of the processes of biomineralization and also to aid our interpretation of any environmental data recorded within biomineral structures for which we rely on proxies such as minor elements and stable isotopes composition.

The bimineralic *Mytilus edulis* shell has an inevitably higher magnesium concentration in the outer calcite layer than in the inner aragonite nacre layer, e.g., 272. Crystal-

lography and inorganic processes are insufficient to explain the magnesium concentration in *M. edulis* shells, since *Mytilus edulis* calcite contains about 5% of the Mg predicted from wholly inorganic experiments.[21] *M. edulis* controls the concentration of magnesium that is incorporated in the shell via physiological fractionation that is effective up until magnesium concentrations in great excess of normal seawater.[21] In experiments using semiartificial seawater with a range of trace element concentrations, Lorens and Bender[273] demonstrated that the concentration of magnesium in *M. edulis* shells increases exponentially in calcite and linearly in aragonite when magnesium concentrations in solution exceeds that of normal seawater.[273] Strontium/calcium ratios in *M. edulis* calcite and aragonite were linearly proportional to the Sr/Ca ratio within the solution, and Na/Ca and S/Ca ratios covary with Mg/Ca.[273] It is suggested that monovalent sodium ions are adsorbed on the calcium carbonate crystal surface.[273] In wild-type *M. edulis*, sodium concentration decreases throughout the calcite layer from the outer part to the polymorph interface, where sodium concentrations increase and remain constant throughout the nacreous aragonite layer.[272] The decrease in sodium concentration throughout the calcite layer suggests that the sodium reservoir is being depleted through time, which would invoke the Doerner−Hoskins law[274] as suggested by Lorens[22] to explain situations where crystal growth depletes the reservoir, resulting in heterogeneous distribution of trace elements in the resultant crystal. However, in the aragonite layer, the sodium concentration recovers to that of the initial concentration in calcite.[272] Sodium distribution in *M. edulis* may result from changes in the rate of crystal growth with a possible decrease in calcite growth rate, resulting in an exclusion of sodium, as growth approaches the polymorph interface. There is certainly a refinement in crystallographic alignment of the calcite fibers from the outer calcite to the boundary between calcite and aragonite,[272] which may support the idea of a kinetic influence on sodium incorporation. However, the fact that magnesium concentrations increase throughout calcite growth and then decrease rapidly at the polymorph interface[272] further complicates this, since increased magnesium concentration would not be expected in calcite growing more slowly. One possible explanation is that the influence of crystal growth rate on the magnesium partition coefficient is converse to that of sodium as for strontium and manganese.[22] Vander Putten et al.[275] concluded that, in *M. edulis* calcite, there are cyclical variations with annual periodicities in Mg, Mn, Sr, Ba, and Pb concentrations. The fact that Mg concentration only covaries with water temperature during the Spring phytoplankton bloom, and not throughout the year, is an illustration of the influence of factors other than water temperature on such environmental proxies.[275] It has been suggested that the distribution of magnesium is a consequence of the metabolic activity of the mantle cells, with high magnesium and sulfur concentrations resulting from highly metabolically active cells.[276,277] Studies of nonbiogenic calcite indicate that, where the carbonate of calcite is substituted by sulfate, the resultant lattice distortions enable more magnesium to be accommodated in the calcite lattice.[278] Thus, in order to understand any relationship between sulfur and magnesium in carbonate biominerals, it is important to determine the nature of the sulfur component. Is sulfur present as an organic component such as acidic sulfated polysaccharides that have been detected in several carbonate biominerals including

molluscs,[127,258,279] corals[126] and avian eggshells,[280] or is it inorganic structurally substituted sulfate (SSS)[281] that enables magnesium to be accommodated more readily?[282]

Problems with Mg/Ca ratios as a proxy for water temperature were also encountered by Freitas et al.[283] studying the king scallop *Pecten maximus*, where there is an inverse relationship between shell Mg/Ca ratio and temperature during Autumn to early Spring (October to March−April). Data on the Sr/Ca ratio of *P. maximus*[283] supports the observation that strontium incorporation is influenced by kinetic effects and is, in fact, a potential proxy for calcification rate.[284]

Checa et al.[285] induced aragonite formation in four species of calcite-producing bivalves by cultivating them in artificial seawater with high Mg/Ca molar ratios in the range 8.3−9.2 when the current value for seawater is 5.2. The scallop *Chlamys varia*, the oyster *Ostrea edulis*, the saddle oyster *Anomia ephippium*, and the mussel *Mytilus edulis* all produced aragonite on the interior shell surface. Some individuals of *C. varia* also increased in length during the cultivation and produced high Mg-calcite at these margins, suggesting that the cells of the marginal mantle were able to maintain the polymorph despite the high magnesium concentrations in the artificial seawater.[285]

Although there is some concern about minor element proxies, such as Mg/Ca ratios in bivalves, being influenced by factors other than seawater temperature,[275,283] the use of stable isotopes such as $\delta^{18}O$ seems much more promising. In *Mytilus edulis*, calcite $\delta^{18}O$ is in oxygen isotope equilibrium with ambient seawater and is not influenced by ontogenetic factors such as changes in growth rate.[286] In a large survey of 14 species of molluscs including Bivalvia, Gastropoda, and Polyplacophora from Martinique, Lécuyer et al.[287] concluded that vital effects were negligible and that there was a direct relationship between ambient water temperature and $\delta^{18}O$ of both calcite and aragonite. The suitability of $\delta^{18}O$ as a proxy for ambient seawater temperature results in investigations of varied environments such as deep-sea hydrothermal vents[288] and ice-melt runoff in Antarctica.[289]

8. Concluding Remarks

The complexity of the chemico-structural relationships within biominerals is only too apparent. In cases where our knowledge is more advanced, such as with molluscan proteins, then common underlying principles become evident. In searching for common mechanisms, one approach may be to consider commonality in periostracum-encased phyla where biomineralization is initiated on the organic template of the periostracum. On the other hand, coccolithophores and foraminiferans are devoid of a periostracum and instead nucleate biominerals within intracellular vesicles.

Although, in one sense, the materials appear simple, we have to remember that at least 550 million years of evolution has evolved a highly complex mechanism that does the job with extreme efficiency. Perhaps a parallel could be drawn with photosynthesis, where the outward simplicity of the leaf, algae, or bacteria belies the immensely regulated, organized, and efficient way photosynthesis takes place. The chromophores that are the business end of the photosynthetic process are assembled and placed precisely on the protein scaffold. We, therefore, should not be surprised that, in studying biomineralization, we engage the simple complexity of Nature.

10. References

(1) Gordon, H. R.; Du, T. *Limnol. Oceanogr.* **2001**, *46*, 1438.
(2) Gordon, H. R. *Appl. Opt.* **2006**, *27*, 7166.
(3) Svensen, Ø.; FretteØ.; Erga, S. R. *Appl. Opt.* **2007**, *46*, 5762.
(4) Price, L. L.; Yin, K.; Harrison, P. J. *J. Exp. Mar. Biol. Ecol.* **1998**, *223*, 223.
(5) Aizenberg, J.; Tkachenko, A.; Weiner, S.; Addadi, L.; Hendler, G. *Nature* **2001**, *412*, 819.
(6) Sundar, V. C.; Yablon, A. D.; Grazul, J. L.; Ilan, M.; Aizenberg, J. *Nature* **2003**, *424*, 899.
(7) Aizenberg, J.; Sundar, V. C.; Yablon, A. D.; Weaver, J. C.; Chen, G. *Proc. Natl. Acad. Sci. U. S. A.* **2004**, *101*, 3358.
(8) Lowenstam, H. A.; Weiner, S. *On Biomineralization*; Oxford University Press: New York, 1989.
(9) Pokroy, B.; Fitch, A. N.; Lee, P. L.; Quintana, J. P.; Caspi, E. N.; Zolotoyabko, E. *J. Struct. Biol.* **2006**, *153*, 145.
(10) Lee, M. R.; Torney, C.; Owen, A. W. *Palaeontology* **2007**, *50*, 1031.
(11) Clarkson, E.; Levi-Setti, R.; Horvath, G. *Arthropod. Struct. Dev.* **2006**, *35*, 247.
(12) Robach, J. S.; Stock, S. R.; Veis, A. *J. Struct. Biol.* **2006**, *155*, 87.
(13) Parkinson, D.; Curry, G. B.; Cusack, M.; Fallick, A. E. *Chem. Geol.* **2005**, *219*, 193.
(14) Carpenter, S. J.; Lohmann, K. C. *Geochim. Cosmochim. Acta* **1995**, *59*, 3748.
(15) Brand, U. *Chem. Geol.* **2004**, *204*, 23.
(16) Allison, N.; Finch, A. A. *Geochem. Geophy. Geosy.* **2004**, 5.
(17) Meibom, A.; Stage, M.; Wooden, J.; Constantz, B. R.; Dunbar, R. B.; Owen, A.; Grumet, N.; Bacon, C. R.; Chamberlain, C. P. *Geophys. Res. Lett.* **2003**, *30*, 1.
(18) Bentov, S.; Erez, J. *Geology* **2005**, *33*, 841.
(19) Elderfield, H.; Yu, J.; Anand, P.; Kiefer, T.; Nyland, B. *Earth Planet. Sci. Lett.* **2006**, *250*, 633.
(20) Reeder, R. J. *Rev. Mineral. Geochem.* **1983**, *11*, 1.
(21) Lorens, R. B.; Bender, M. L. *Nature* **1977**, *269*, 293.
(22) Lorens, R. B. *Geochim. Cosmochim. Acta* **1981**, *45*, 553.
(23) Reeder, R. J.; Paquette, J. *Sediment. Geol.* **1989**, *65*, 239.
(24) Paquette, J.; Reeder, R. J. *Geology* **1990**, *18*, 1244.
(25) Paquette, J.; Reeder, R. J. *Geochim. Cosmochim. Acta* **1995**, *59*, 735.
(26) Wasylenki, L. E.; Dove, P. M.; De Yoreo, J. J. *Geochim. Cosmochim. Acta* **2005**, *69*, 4227.
(27) Reeder, R. J.; Grams, J. C. *Geochim. Cosmochim. Acta* **1987**, *51*, 187.
(28) Dickson, J. A. D. *Mineral. Mag.* **1997**, *61*, 243.
(29) Klein, R. T.; Lohmann, K. C. *Geology* **1995**, *23*, 633.
(30) Reeder, R. J.; Valley, J. W.; Graham, C. M.; Eiler, J. M. *Geochim. Cosmochim. Acta* **1997**, *61*, 5057.
(31) Cusack, M.; Fraser, A. C.; Stachel, T. *Comp. Biochem. Physiol. B.* **2003**, *134*, 63.
(32) Dalbeck, P.; Cusack, M. *Cryst. Growth Des.* **2006**, *6*, 2558.
(33) Urey, H. C. *J. Chem. Soc* **1947**, *108*, 562.
(34) Epstein, S.; Buchsbaum, R.; Lowenstam, H. A.; Urey, H. C. *B. Geol. Soc. U.S.A.* **1953**, *64*, 1315.
(35) Lowenstam, H. A. *J. Geol.* **1961**, *69*, 241.
(36) Beniash, E.; Aizenberg, J.; Addadi, L.; Weiner, S. *Proc. R. Soc. Lond. B.* **1997**, *264*, 461.
(37) Raz, S.; Hamilton, P. C.; Wilt, F. H.; Weiner, S.; Addadi, L. *Adv. Funct. Mater.* **2003**, *13*, 480.
(38) Politi, Y.; Arad, T.; Klein, E.; Weiner, S.; Addadi, L. *Science* **2004**, *306*, 1161.
(39) Becker, A.; Ziegler, A.; Epple, M. *Dalton Trans.* **2005**, *10*, 1814.
(40) Weiss, I. M.; Tuross, N.; Addadi, L.; Weiner, S. *J. Exp. Zool.* **2002**, *293*, 478.
(41) Nassif, N.; Pinna, N.; Gehrke, N.; Antonietti, M.; Jager, C.; Colfen, H. *Proc. Natl. Acad. Sci. U. S. A.* **2005**, *102*, 12653.
(42) Jager, C.; Colfen, H. *CrystEngComm* **2007**, *9*, 1237.
(43) Aizenberg, J.; Weiner, S.; Addadi, L. *Connect. Tiss. Res.* **2003**, *44*, 20.
(44) Addadi, L.; Raz, S.; Weiner, S. *Adv. Mater.* **2003**, *15*, 959.
(45) Aizenberg, J.; Lambert, G.; Weiner, S.; Addadi, L. *J. Am. Chem. Soc.* **2002**, *124*, 32.
(46) Loste, E.; Wilson, R. M.; Seshadri, R.; Meldrum, F. C. *J. Cryst. Growth* **2003**, *254*, 206.

(47) Xingguo, C.; Varona, P. L.; Olszta, M. J.; Gower, L. B. *J. Cryst. Growth* **2007**, *307*, 395.
(48) Politi, Y.; Mahamid, J.; Goldberg, H.; Weiner, S.; Addadi, L. *CrystEngComm* **2007**, *9*, 1171.
(49) Gehrke, N.; Nassif, N.; Pinna, N.; Antonietti, M.; Gupta, H. S.; Colfen, H. *Chem. Mater.* **2005**, *17*, 6514.
(50) Hasse, B.; Ehrenberg, H.; Marxen, J. C.; Becker, W.; Epple, M. *Chem.-Eur. J.* **2000**, *6*, 3679.
(51) Politi, Y.; Levi-Kalisman, Y.; Raz, S.; Wilt, F.; Addadi, L.; Weiner, S.; Sagi, I. *Adv. Funct. Mater.* **2006**, *16*, 1289.
(52) Cohen, A. L.; McConnaughey, T. A. *Rev. Mineral. Geochem.* **2003**, *54*, 151.
(53) Benayahu, Y.; Jeng, M.-S.; Perkol-Finkel, S.; Dai, C.-F. *Zool. Stud.* **2004**, *43*, 548.
(54) Cuif, J. P.; Dauphin, Y. *Biogeosciences* **2005**, *2*, 61.
(55) Blamart, D.; Rollion-Bard, C.; Meibom, A.; Cuif, J. P.; Juillet-Leclerc, A.; Dauphin, Y. *Geochem. Geophys. Geosyst.* **2007**, *8*, Q12001.
(56) Perrin, C. *Coral Reefs* **2003**, *22*, 109.
(57) Cuif, J. P.; Dauphin, Y. *J. Struct. Biol.* **2005**, *150*, 319.
(58) Cuif, J. P.; Dauphin, Y. *Palaeontol. Z.* **1998**, *72*, 257.
(59) Dauphin, Y.; Cuif, J. P.; Massard, P. *Chem. Geol.* **2006**, *231*, 26.
(60) Dodge, R. E.; Vaisnys, J. R. *Nature* **1975**, *258*, 706.
(61) Fang, L.-S.; Chou, Y.-C. *Coral Reefs* **1992**, *11*, 187.
(62) Matthews, B. J. H.; Jones, A. C.; Theodorou, N. K.; Tudhope, A. W. *Mar. Chem.* **1996**, *55*, 317.
(63) Enmar, R.; Stein, M.; Bar-Matthews, M.; Sass, E.; Katz, A.; Lazar, B. *Geochim. Cosmochim. Acta* **2000**, *64*, 3123.
(64) Cohen, A. L.; Gaetani, G. A.; Lundalv, T.; Corliss, B. H.; George, R. Y. *Geochem. Geophy. Geosy.* **2006**, *7*, Q12004.
(65) Fukuda, I.; Ooki, S.; Fujita, T.; Murayama, E.; Nagasawa, H.; Isa, Y.; Watanabe, T. *Biochem. Biophys. Res. Commun.* **2003**, *304*, 11.
(66) Watanabe, T.; Fukuda, I.; China, K.; Isa, Y. *Comp. Biochem. Physiol. B.* **2003**, *136*, 767.
(67) Puverel, S.; Tambutte, E.; Pererra-Mouries, L.; Zoccola, D.; Allemand, D.; Tambutte, S. *Comp. Biochem. Physiol. B.* **2005**, *141*, 480.
(68) Cuif, J.-P.; Dauphin, Y.; Gautret, P. *Int. J. Earth Sci.* **1999**, *88*, 582.
(69) Addadi, L.; Weiner, S. *Proc. Natl. Acad. Sci. U. S. A.* **1985**, *82*, 4110.
(70) Albeck, S.; Aizenberg, J.; Addadi, L.; Weiner, S. *J. Am. Chem. Soc.* **1993**, *115*, 11691.
(71) Bedouet, L.; Schuller, M. J.; Marin, F.; Milet, C.; Lopez, E.; Giraud, M. *Comp. Biochem. Physiol. B.* **2001**, *128*, 389.
(72) Moradian-Oldak, J.; Frolow, F.; Addadi, L.; Weiner, S. *Proc. R. Soc. Lond. B.* **1992**, *247*, 47.
(73) Furedimilhofer, H.; Moradianoldak, J.; Weiner, S.; Veis, A.; Mintz, K. P.; Addadi, L. *Connect. Tiss. Res.* **1994**, *30*, 251.
(74) Falini, G.; Albeck, S.; Weiner, S.; Addadi, L. *Science* **1996**, *271*, 67.
(75) Oldberg, A.; Franzen, A.; Heinegard, D. *Proc. Natl. Acad. Sci. U. S. A.* **1986**, *83*, 8819.
(76) Goldberg, H.; Warner, K. J.; Li, M. C.; Hunter, G. K. *Connect. Tiss. Res.* **2001**, *42*, 25.
(77) Tsukamoto, D.; Sarashina, I.; Endo, K. *Biochem. Biophys. Res. Commun.* **2004**, *320*, 1175.
(78) Rahman, M. A.; Isa, Y. *J. Exp. Mar. Biol. Ecol.* **2005**, *321*, 71.
(79) Rahman, M. A.; Isa, Y.; Uehara, T. *Proteomics* **2005**, *5*, 885.
(80) Allison, N. *Geochim. Cosmochim. Acta* **1996**, *60*, 3457.
(81) Meibom, A.; Cuif, J.-P.; Hillion, F.; Constantz, B. R.; Juillet-Leclerc, A.; Dauphin, Y.; Watanabe, T.; Dunbar, R. B. *Geophys. Res. Lett.* **2004**, *31*, 1.
(82) Meibom, A.; Yurimoto, H.; Cuif, J.-P.; Domart-Coulon, I.; Houlbreque, F.; Constantz, B.; Dauphin, Y.; Tambutte, E.; Tambutte, S.; Allemand, D.; Wooden, J.; Dunbar, R. *Geophys. Res. Lett.* **2006**, *33*, 1.
(83) Allison, N.; Finch, A. A.; Newville, M.; Sutton, S. R. *Geochim. Cosmochim. Acta* **2005**, *69*, 3801.
(84) Cohen, A. L.; Ownes, K. E.; Layne, G. D.; Shimiizu, N. *Science* **2002**, *269*, 331.
(85) Cohen, A. L.; Sohn, R. A. *Geophys. Res. Lett.* **2004**, *31*, . doi: 10.1029/2004GL020600.
(86) Fallon, S. J.; McCulloch, M. T.; van Woesik, R.; Sinclair, D. J. *Earth Planet. Sci. Lett.* **1999**, *172*, 221.
(87) Hart, S. R.; Cohen, A. L. *Geochim. Cosmochim. Acta* **1996**, *60*, 3075.
(88) Gagnon, A. C.; Adkins, J. F.; Fernandez, D. P.; Robinson, L. F. *Earth Planet. Sci. Lett.* **2007**, *261*, 280.
(89) Gabitov, R. I.; Cohen, A. L.; Gaetani, G. A.; Holcomb, M.; Watson, E. B. *Geochim. Cosmochim. Acta* **2006**, *70*, A187.
(90) Cohen, A. L.; Layne, G. D.; Hart, S. R.; Lobel, P. S. *Paleoceanography* **2001**, *16*, 20.
(91) Inoue, M.; Suzuki, A.; Nohara, M.; Hibino, K.; Kawahata, H. *Geophys. Res. Lett.* **2007**, *34*, 1.
(92) Watson, E. B.; Yan Liang, Y. *Am. Mineral.* **1995**, *80*, 1179.
(93) Watson, E. B. *Geochim. Cosmochim. Acta* **1996**, *60*, 5013.
(94) Gaetani, G. A.; Cohen, A. L. *Geochim. Cosmochim. Acta* **2006**, *70*, 4617.
(95) Sinclair, D. J.; Williams, B.; Risk, M. *Geophys. Res. Lett.* **2006**, *33*.
(96) McConnaughey, T. A. *Coral Reefs* **2003**, *22*, 316.
(97) Rollion-Bard, C.; Blamart, D.; Cuif, J. P.; Juillet-Leclerc, A. *Coral Reefs* **2003**, *22*, 405.
(98) Al-Moghrabi, S. M.; Al-Horani, F. A.; deBeer, D. 8th International Symposium on Biomineralization, Kurukawa, Japan, 2001; p 45.
(99) Lear, C. H.; Rosenthal, Y.; Slowey, N. *Geochim. Cosmochim. Acta* **2002**, *66*, 3375.
(100) Rosenthal, Y.; Boyle, E. A.; Slowey, N. *Geochim. Cosmochim. Acta* **1997**, *61*, 3633.
(101) Fontanier, C.; Mackensen, A.; Jorissen, F. J.; Anschutz, P.; Licari, L.; Griveaud, C. *Mar. Micropaleontol.* **2006**, *58*, 159.
(102) Elderfield, H.; Cooper, M.; Ganssen, G. *Geochem. Geophys. Geosyst.* **2000**, *1*, 1999GC000031.
(103) Eggins, S.; DeDecker, P.; Marshall, J. *Earth Planet. Sci. Lett.* **2003**, *212*, 219.
(104) Ishikawa, S.; Oda, M. *Mar. Micropaleontol.* **2007**, *63*, 143.
(105) Armstrong, H.; Brasier, M. D. *Microfossils*, second ed.; Blackwell Publishing: Cambridge, MA, 2005.
(106) Erez, J. *Rev. Mineral. Geochem.* **2003**, *54*, 115.
(107) Wetmore, K. L.; Plotnick, R. E. *J. Foraminifer. Res.* **1992**, *22*, 1.
(108) Toler, S. K.; Hallock, P.; Schijf, J. *Mar. Micropaleontol.* **2001**, *43*, 199.
(109) Talge, H. K.; Hallock, P. *Mar. Micropaleontol.* **1995**, *26*, 107.
(110) Robbins, L. L.; Brew, K. *Geochim. Cosmochim. Acta* **1990**, *54*, 2285.
(111) Weiner, S.; Erez, J. *J. Foraminifer. Res.* **1984**, *14*, 206.
(112) Haugen, J. E.; Sejrup, H. P.; Vogt, N. B. *J. Foraminifer. Res.* **1989**, *19*, 38.
(113) Robbins, L. L.; Healywilliams, N. *J. Foraminifer. Res.* **1991**, *21*, 159.
(114) Robbins, L. L.; Donachy, J. E. *ACS Symp. Ser.* **1991**, *444*, 139.
(115) Robbins, L. L.; Toler, S. K.; Donachy, J. E. *Lethaia* **1993**, *26*, 269.
(116) Anand, P.; Elderfield, H. *Geochem. Geophys. Geosyst.* **2005**, *6*, Q11D15.
(117) Bentov, S.; Erez, J. *Geochem. Geophys. Geosyst.* **2006**, *7*, Q01P08.
(118) Segev, E.; Erez, J. *Geochem. Geophys. Geosyst.* **2006**, *7*, Q02P09.
(119) Kunioka, D.; Shirai, K.; Takahata, N.; Sano, Y.; Toyofuku, T.; Ujiie, Y. *Geochem. Geophys. Geosyst.* **2006**, *7*, Q12P20.
(120) Elderfield, H.; Vautravers, M.; Cooper, M. *Geochem. Geophys. Geosyst.* **2002**, *3*, 1052.
(121) Yu, J.; Day, J.; Greaves, M.; Elderfield, H. *Geochem. Geophys. Geosyst.* **2005**, *6*, Q08P01.
(122) Brown, S. J.; Elderfield, H. *Paleoceanography* **1996**, *11*, 543.
(123) Nouet, J.; Bassinot, F. *Geochem. Geophys. Geosyst.* **2007**, *8*, Q10007.
(124) Corliss, B. H.; Sun, X.; Brown, C. W.; Showers, W. J. *Deep-Sea Res. Part I Oceanogr. Res. Pap.* **2006**, *53*, 740.
(125) Young, J. R.; Davis, S. A.; Bown, P. R.; Mann, S. *J. Struct. Biol.* **1999**, *126*, 195.
(126) Cuif, J. P.; Dauphin, Y.; Doucet, J.; Salome, M.; Susini, J. *Geochim. Cosmochim. Acta* **2003**, *67*, 75.
(127) Dauphin, Y.; Cuif, J. P.; Salome, C.; Susini, J. *Am. Mineral.* **2005**, *90*, 1748.
(128) Marsh, M. E.; Chang, D.-K.; King, G. C. *J. Biol. Chem.* **1992**, *267*, 20507.
(129) Marsh, M. E. *Protoplasma* **1994**, *177*, 108.
(130) Marsh, M. E.; Ridall, A. L.; Azadi, P.; Duke, P. J. *J. Struct. Biol.* **2002**, *139*, 39.
(131) Marsh, M. E. *Comp. Biochem. Physiol. B.* **2003**, *136*, 743.
(132) Klaveness, D. *Protistologica* **1976**, *12*, 217.
(133) Mann, S.; Sparks, N. H. C. *Proc. R. Soc. Lond. B.* **1988**, *234*, 441.
(134) Fichtinger-Schepman, A. M. J.; Kamerling, J. P.; Versluis, C.; Vliegenthart, J. F. G. *Carbohydr. Res.* **1981**, *93*, 105.
(135) Corstjens, P.; van der Kooij, A.; Linschooten, C.; Brouwers, G. J.; Westbroek, P.; de Vrind-de Jong, E. W. *J. Phycol.* **1998**, *34*, 622.
(136) Kawasaki, H.; Kretsinger, R. H. *Protein Profile* **1994**, *1*, 343.
(137) Young, J. R.; Henriksen, K. *Rev. Mineral. Geochem.* **2003**, *54*, 189.
(138) Ozaki, N.; Sakuda, S.; Nagasawa, H. *Biosci. Biotechnol. Biochem.* **2001**, *65*, 2330.
(139) Mitchell, S. F.; Ball, J. D.; Crowley, S. F.; Marshall, J. D.; Paul, C. R. C.; Veltkamp, C. J.; Samir, A. *Geology* **1997**, *25*, 691.
(140) Paull, C. K.; Balch, W. M. *Deep-Sea Res. Part I Oceanogr. Res. Pap.* **1994**, *41*, 223.
(141) Ziveri, P.; Stoll, H.; Probert, I.; Klass, C.; Geisen, M.; Ganssen, G.; Young, J. *Earth Planet. Sci. Lett.* **2003**, *210*, 137.
(142) Stanley, S. M.; Hardie, L. A. *Palaeogeogr. palaeocl.* **1998**, *144*, 3.
(143) Herfort, L.; Loste, E.; Meldrum, F.; Thake, B. *J. Struct. Biol.* **2004**, *148*, 307.
(144) Stoll, H. M.; Klaas, C. M.; Probert, I.; Encinar, J. R.; Alonso, J. I. G. *Global Planet. Change* **2002**, *34*, 153.
(145) Stoll, H. M.; Schrag, D. P. *Geochem. Geophys. Geosyst.* **2000**, *1*, 1.

(146) Stoll, H. M.; Ziveri, P.; Geisen, M.; Probert, I.; Young, J. R. *Philos. Trans. R. Soc. Lond. A* **2002**, *360*, 719.

(147) Stoll, H. M.; Rosenthal, Y.; Falkowski, P. *Geochim. Cosmochim. Acta* **2002**, *66*, 927.

(148) Rickaby, R. E. M.; Bard, E.; Sonzogni, C.; Rostek, F.; Beaufort, L.; Barker, S.; Rees, G.; Schrag, D. P. *Earth Planet. Sci. Lett.* **2007**, *253*, 83.

(149) Stoll, H. M.; Bains, S. *Paleoceanography* **2003**, *18*, 1049.

(150) Stoll, H. M.; Shimizu, N.; Archer, D.; Ziveri, P. *Earth Planet. Sci. Lett.* **2007**, *258*, 192.

(151) Williams, A.; Carlson, S. J.; Brunton, C. H. C.; Holmer, L. E.; Popov, L. *Philos. Trans. R. Soc. Lond. B.* **1996**, *351*, 1171.

(152) Mackay, S.; Mackinnon, D. I.; Williams, A. *Lethaia* **1994**, *26*, 367.

(153) Jope, M. In *Treatise on Invertebrate Paleontology, Part H, Brachiopoda*; Moore, R. C., Ed.; The University of Kansas Press and the Geological Society of America: Lawrence, KS, 1965; Vol. 1.

(154) Jope, M. *Comp. Biochem. Physiol. B.* **1967**, *20*, 601.

(155) Jope, M. *Comp. Biochem. Physiol. B.* **1969**, *30*, 209.

(156) Jope, M. *Comp. Biochem. Physiol. B.* **1969**, *30*, 225.

(157) Jope, M. *Comp. Biochem. Physiol. B.* **1973**, *45B*, 17.

(158) Jope, M. *Comp. Biochem. Physiol. B.* **1979**, *63B*, 163.

(159) Cusack, M. *Bulletin de I'Institut Océanography, Monaco* **1996**, *14*, 271.

(160) Leveque, I.; Cusack, M.; Davis, S. A.; Mann, S. *Angew. Chem., Int. Ed.* **2004**, *43*, 885.

(161) Williams, A.; Cusack, M.; Mackay, S. *Philos. Trans. R. Soc. Lond. B.* **1994**, *346*, 223.

(162) Williams, A.; Cusack, M.; Buckman, J. O. *Philos. Trans. R. Soc. Lond. B.* **1998**, *353*, 2005.

(163) Williams, A.; Cusack, M.; Brown, K. *Proc. R. Soc. Lond. B.* **1999**, *266*, 1601.

(164) Cusack, M.; Laing, J. H.; Brown, K.; Walton, D. *Trends Comp. Biochem. Physiol. B.* **2000**, *6*, 47.

(165) Cusack, M.; Williams, A. *Palaeontology* **2001**, *44*, 875.

(166) Cusack, M.; Curry, G.; Clegg, H.; Abbott, G. *Comp. Biochem. Physiol. B.* **1992**, *102*, 93.

(167) Cusack, M.; Williams, A. In *Brachiopods Past and Present*; Brunton, C. H. C., Cocks, L. R. M., Long, S. L., Ed.; Taylor & Francis: London, 2001.

(168) Gaspard, D.; Marie, B.; Guichard, N.; Luquet, G.; Marin, F. Biomineralization: From Paleontology to Materials Science. Proceedings of the 9th International Symposium on Biomineralization, Santiago, Chile, 2007; p 193.

(169) Lowenstam, H. A.; Weiner, S. *Proc. Natl. Acad. Sci. U. S. A.* **1992**, *89*, 10573.

(170) Kelly, P. G.; Oliver, P. T. P.; Pautard, F. G. E. *Proc 2nd Eur Symp Calcified Tissue* **1965**, 337.

(171) Watabe, N.; Pan, C.-M. *Am. Zool.* **1984**, *24*, 977.

(172) Legeros, R. Z.; Pan, C. M.; Suga, S.; Watabe, N. *Calcif. Tissue Int.* **1985**, *37*, 98.

(173) Pan, C.-M.; Watabe, N. *J. Exp. Mar. Biol. Ecol.* **1988**, *119*, 43.

(174) Cusack, M.; Williams, A.; Buckman, J. O. *Palaeontology* **1999**, *42*, 799.

(175) Iijima, M.; Moriwaki, Y.; Doi, Y.; Kuboki, Y. *Jpn. J.Oral Biol* **1988**, *30*, 20.

(176) Iijima, M.; Moriwaki, Y. *Calcif. Tissue Int.* **1990**, *47*, 237.

(177) Cusack, M.; Walton, D.; Curry, G. B. In *Introduction. Treatise on Invertebrate Paleontology*; Kaesler, R., Ed.; Geol. Soc. Am. & Univ. Kansas Press.: New York and Lawrence, 1997; Vol. 1.

(178) Perry, C. C.; Wilcock, J. R.; Williams, R. J. P. *Experientia* **1998**, *44*, 638.

(179) Lüter, C. *Biol. Lett.* **2004**, *271*, S465.

(180) Westbroek, P.; de Jong, E. W.; van der Wal, P.; Borman, A. H.; deVrind, J. P. M.; Kok, D.; de Bruijn, W. C.; Parker, S. B. *Philos. Trans. R. Soc. Lond. B.* **1984**, *304*, 435.

(181) Williams, A. *Palaeontology* **2003**, *46*, 67.

(182) Balthasar, U. W. E. *Palaeontology* **2007**, *50*, 1319.

(183) Cusack, M.; Williams, A. In *Treatise on Invertebrate Paleontology, Part H, Brachiopoda*; Kaesler, R., Ed.; Geol. Soc. Am. & Univ. Kansas: New York, 2007; Vol. 6.

(184) England, J.; Cusack, M.; Lee, M. R. *Lethaia* **2007**, *40*, 2.

(185) England, J.; Cusack, M.; Dalbeck, P.; Perez-Huerta, A. *Cryst. Growth Des.* **2007**, *7*, 307.

(186) Taylor, P. D.; Weedon, M. J. *Zool. J. Linn. Soc.* **2000**, *128*, 337.

(187) Schmahl, W. W.; Griesshaber, E.; Neuser, R.; Lenze, A.; Job, R.; Brand, U. *Eur. J. Mineral* **2004**, *16*, 693.

(188) Cusack, M.; Parkinson, D.; Perez-Huerta, A.; England, J.; Curry, G. B.; Fallick, A. E. *Earth Env. Sci. Trans. Roy. Soc. Edin.* ,

(189) Pérez-Huerta, A.; Cusack, M.; Jeffries, T.; Williams, T. *Chem. Geol.* **2008**, *247*, 229.

(190) Veizer, J.; Fritz, P.; Jones, B. *Geochim. Cosmochim. Acta* **1986**, *50*, 1679.

(191) Korte, C.; Jasper, T.; Kozur, H. W.; Veizer, J. *Palaeogeogr. palaeocl.* **2005**, *224*, 333.

(192) Brand, U. *Chem. Geol.* **2004**, *204*, 23.

(193) Adlis, D. S.; Grossman, E. L.; Yancey, T. E.; McLerran, R. D. *Palaios* **1988**, *3*, 487.

(194) Grossman, E. L.; Zhang, C.; Yancey, T. E. *GSA Bull.* **1991**, *103*, 953.

(195) Grossman, E. L.; Mii, H.-S.; Yancey, T. E. *GSA Bull.* **1993**, *105*, 1284.

(196) Azmy, K.; Veizer, J.; Jin, J.; Copper, P.; Brand, U. *Can. J. Earth Sci* **2006**, *43*, 281.

(197) Auclair, A.-C.; Joachimski, M. M.; Lécuyer, C. *Chem. Geol.* **2003**, *202*, 59.

(198) Rodland, D. L.; Kowalewski, M.; Atudorei, V.; Sharp, Z. D.; Dettman, D. L. *GSA Abs.* **2001**,

(199) Barthelat, F.; Espinosa, H. D. SEM Annual Conference and Exposition on Experimental and Applied Mecahnics, Charlotte, NC, 2003.

(200) Jackson, A. P.; Vincent, J. F. V.; Turner, R. M. *J. Mater. Sci.* **1990**, *25*, 3173.

(201) Taylor, J. D. *Palaeontology* **1973**, *16*, 519.

(202) Marin, F.; Luquet, G.; Marie, B.; Medakovic, D. *Curr. Top. Dev. Biol.* **2008**, *80*, 209.

(203) Sarashina, I.; Endo, K. *Paleontol. Res.* **2006**, *10*, 311.

(204) Zhang, C.; Zhang, R. *Mar. Biotechnol.* **2006**, *8*, 572.

(205) Kobayashi, I.; Samata, T. *Mater. Sci. Eng., C* **2006**, *26*, 692.

(206) Gotliv, B. A.; Kessler, N.; Sumerel, J. L.; Morse, D. E.; Tuross, N.; Addaddi, L.; Weiner, S. *ChemBioChem* **2005**, *6*, 304.

(207) Sarashina, I.; Endo, K. *Am. Mineral.* **1998**, *83*, 1510.

(208) Sarashina, I.; Endo, K. *Mar. Biotechnol.* **2001**, *3*, 362.

(209) Maurera, P.; Hohenesterb, E.; Engelc, J. *Curr. Opin. Cell Biol.* **1996**, *8*, 609.

(210) Sudo, S.; Fujikawa, T.; Nagakura, T.; Ohkubo, T.; Sakaguchi, K.; Tanaka, M.; Nakashima, K.; Takahashi, T. *Nature* **1997**, *387*, 563.

(211) Takeuchi, T.; Endo, K. *Mar. Biotechnol.* **2005**, *8*, 1436.

(212) Inoue, H.; Ozaki, N.; Nagasawa, H. *Biosci. Biotechnol. Biochem.* **2001**, *65*, 1840.

(213) Jones, L. R.; Zhang, L.; Sanborn, K.; Jorgensen, A. O.; Kelley, J. *J. Biol. Chem.* **1995**, *270*, 30787.

(214) Lee, S. W.; Kim, Y. M.; Choi, H. S.; Yang, J. M.; Choi, C. S. *Prot. J.* **2006**, *25*, 288.

(215) Miyamoto, H.; Miyashita, T.; Okushima, M.; Nakano, S.; Morita, T.; Matsushiro, A. *Proc. Natl. Acad. Sci. U. S. A.* **1996**, *93*, 9657.

(216) Miyashita, T.; Takagi, R.; Miyamoto, H.; Matsushiro, A. *Veliger* **2002**, *45*, 250.

(217) Kono, M.; Hayashi, N.; Samata, T. *Biochem. Biophys. Res. Commun.* **2000**, *269*, 213.

(218) Samata, T.; Hayashi, N.; Kono, M.; Hasegawa, K.; Horita, C.; Akera, S. *FEBS Lett.* **1999**, *462*, 225.

(219) Samata, T.; Kono, M.; Hayashi, N.; Oyama, S.; Suganaga, M. In *Biomineralization: Formation, Diversity, Evolution and Application*; Kobayashi, I., Osawa, H., Eds.; Tokai University Press: Kanagawa, Japan, 2003.

(220) Miyashita, T.; Takaki, R.; Okushima, M.; Nakano, S.; Miyamoto, H.; Neshikawa, E.; Matsushiro, A. *Mar. Biotechnol.* **2000**, *2*, 409.

(221) Miyashita, T.; Miyamoto, H.; Matsushiro, A. In *Biomineralization: Formation, Diversity, Evolution and Application*; Kobayashi, I., Osawa, H., Eds.; Tokai University Press: Kanagawa, Japan, 2003.

(222) Yano, M.; Nagai, K.; Morimoto, K.; Miyamoto, H. *Biochem. Biophys. Res. Commun.* **2007**, *362*, 158.

(223) Marin, F.; Corstjens, P.; de Gaulejac, B.; Vrind-De Jong, E. D.; Westbroek, P. *J. Biol. Chem.* **2000**, *275*, 20667.

(224) Marin, F.; de Groot, K.; Westbroek, P. *Protein Expr. Purif.* **2003**, *30*, 246.

(225) Addadi, L.; Joester, D.; Nudelman, F.; Weiner, S. *Chem.-Eur. J.* **2006**, *12*, 981.

(226) Bohm, F.; Joachimski, M. M.; Dullo, W. C.; Eisenhauer, A.; Lehnert, H.; Reitner, J.; Worheide, G. *Geochim. Cosmochim. Acta* **2000**, *64*, 1695.

(227) Wheeler, A. P.; Rusenko, K. W.; Sikes, C. S. In *Chemical aspects of regulation of mineralization*; Sikes, C. S., Wheeler, A. P., Eds.; University of South Alabama Publication Service: Mobile, AL, 1988.

(228) Mouries, L. P.; Almeida, M. J.; Milet, C.; Berland, S.; Lopez, E. *Comp. Biochem. Physiol. B.* **2002**, *132*, 217.

(229) Marin, F.; Amons, R.; Guichard, N.; Stigter, M.; Hecker, A.; Luquet, G.; Layrolle, P.; Alcaraz, G.; Riondet, C.; Westbroek, P. *J. Biol. Chem.* **2005**, *280*, 33895.

(230) Michenfelder, M.; Fu, G.; Lawrence, C.; Weaver, J. C.; Wustman, B. A.; Taranto, L.; Evans, J. S.; Morse, D. E. *Biopolymers.* **2003**, *70*, 522.

(231) Michenfelder, M.; Fu, G.; Lawrence, C.; Weaver, J. C.; Wustman, B. A.; Taranto, L.; Evans, J. S.; Morse, D. E. *Biopolymers.* **2004**, *73*, 291.

(232) Kim, I. W.; Morse, D. E.; Evans, J. S. *Langmuir* **2004**, *20*, 11664.

(233) Wustman, B. A.; Morse, D. E.; Evans, J. S. *Biopolymers* **2004**, *74*, 363.

(234) Fu, G.; Qiu, S. R.; Orme, C. A.; Morse, D. E.; De Yoreo, J. J. *Adv. Mater.* **2005**, *17*, 2678.

(235) Zhang, Y.; Xie, L.; Meng, Q.; Jaing, T.; Pu, R.; Chen, L.; Zhang, R. *Comp. Biochem. Physiol. B.* **2003**, *135*, 565.

(236) Shen, X.; Belcher, A. M.; Hansma, P. K.; Stucky, G. D.; Morse, D. E. *J. Biol. Chem.* **1997**, *272*, 32472.

(237) Smith, B. L.; Schäffer, T. E.; Viani, M.; Thompson, J. B.; Frederick, N. A.; Kindt, J.; Belcher, A. M.; Stucky, G. D.; Morse, D. E.; Hasma, P. K. *Nature* **1999**, *399*, 761.

(238) Wustman, B. A.; Morse, D. E.; Evans, J. S. *Langmuir* **2002**, *18*, 9901.

(239) Wustman, B. A.; Weaver, J. C.; Morse, D. E.; Evans, J. S. *Connect. Tiss. Res.* **2003**, *44*, 10.

(240) Wustman, B. A.; Weaver, J. C.; Morse, D. E.; Evans, J. S. *Langmuir* **2003**, *19*, 9373.

(241) Zhang, B.; Wustman, B. A.; Morse, D.; Evans, J. S. *Biopolymers* **2002**, *63*, 358.

(242) Weiss, I. M.; Kaufmann, S.; Mann, K.; Fritz, M. *Biochem. Biophys. Res. Commun.* **2000**, *267*, 17.

(243) Weiss, I. M.; Gohring, W.; Fritz, M.; Mann, K. *Biochem. Biophys. Res. Commun.* **2001**, *285*, 244.

(244) Mann, K.; Weiss, I. M.; Andre, S.; Gabius, H.-J.; Fritz, M. *Eur. J. Biochem.* **2000**, *267*, 5257.

(245) Treccani, L.; Mann, K.; Heinemann, F.; Fritz, M. *Biophys. J.* **2006**, *91*, 2601.

(246) Mann, K.; Siedler, F.; Treccani, L.; Heinemann, F.; Fritz, M. *Biophys. J.* **2007**, *93*, 1246.

(247) Westbroek, P.; Marin, F. *Nature* **1998**, *392*, 861.

(248) Lamghari, M.; Almeida, M. J.; Berland, S.; Huet, H.; Laurent, A.; Milet, C.; Lopez, E. *Bone* **1999**, *25*, 91S.

(249) Rousseau, M.; Pereira-Mouriés, L.; Almeida, M.-J.; Milet, C. *Comp. Biochem. Physiol.* **2003**, *135*, 1.

(250) Duplat, D.; Gallet, M.; Bedouet, L.; Milet, C.; Brasier, M.; Kamel, S.; Lopez, E. *J. Bone Miner. Res.* **2004**, *19*, S155.

(251) Blank, S.; Arnoldi, M.; Khoshnavaz, S.; Treccani, L.; Kuntz, M.; Mann, K.; Grathwohl, G.; Fritz, M. *J. Microsc.* **2003**, *212*, 280.

(252) Zhang, Y.; Xie, L.; Huang, J.; Liu, X.; Zhang, R. *Biochem. Biophys. Res. Commun.* **2006**, *344*, 735.

(253) Yano, M.; Nagai, K.; Morimoto, K.; Miyamoto, H. *Comp. Biochem. Physiol. B.* **2006**, *144*, 254.

(254) Cartwright, J. H. E.; Checa, A. G. *J. Royal Soc. Interface* **2007**, *4*, 491.

(255) Nudelman, F.; Shimoni, E.; Klein, E.; Rousseau, M.; Bourrat, X.; Lopez, E.; Addadi, L.; Weiner, S. *J. Struct. Biol.* **2008**, *162*, 290.

(256) Nudelman, F.; Chen, H. H.; Goldberg, H. A.; Weiner, S.; Addadi, L. *Faraday Discuss.* **2007**, *136*, 9.

(257) Marie, B.; Luquet, G.; De Barros, J. P. P.; Guichard, N.; Morel, S.; Alcaraz, G.; Bollache, L.; Marin, F. *FEBS J.* **2007**, *274*, 2933.

(258) Nudelman, F.; Gotliv, B. A.; Addadi, L.; Weiner, S. *J. Struct. Biol.* **2006**, *153*, 176.

(259) Pereira-Mouries, L.; Almeida, M. J.; Ribeiro, C.; Peduzzi, J.; Barthelemy, M.; Milet, C.; Lopez, E. *Eur. J. Biochem.* **2002**, *269*, 4994.

(260) Hattan, S. J.; Laue, T. M.; Chasteen, N. D. *J. Biol. Chem.* **2001**, *276*, 4461.

(261) Yin, Y.; Huang, D.; Paine, M. L.; Reinhold, V. N.; Chasteen, N. D. *Abstr. Pap. Am. Chem. Soc.* **2005**, *229*, U228.

(262) Weiner, S.; Traub, W. *FEBS Lett.* **1980**, *111*, 311.

(263) Levi-Kalisman, Y.; Falini, G.; Addadi, L.; Weiner, S. *J. Struct. Biol.* **2001**, *135*, 8.

(264) Lin, A.; Meyers, M. A. *Mater. Sci. Eng., A.* **2005**, *390*, 27.

(265) Gotliv, B.-A.; Kessler, N.; Sumerel, J. L.; Morse, D. E.; Tuross, N.; Addadi, L.; Weiner, S. *ChemBioChem* **2005**, *6*, 304.

(266) Belcher, A. M.; Wu, X. H.; Christensen, R. J.; Hansma, P. K.; Stucky, G. D.; Morse, D. E. *Nature* **1996**, *381*, 56.

(267) Rousseau, M.; Lopez, E.; Coute, A.; Mascarel, G.; Smith, D. C.; Naslain, R.; Bourrat, X. *J. Struct. Biol.* **2005**, *149*, 149.

(268) Checa, A. G.; Rodriguez-Navarro, A. B. *Biomaterials* **2005**, *26*, 1071.

(269) DiMasi, E.; Sarikaya, M. *J. Mater. Res.* **2004**, *19*, 1471.

(270) Hou, W. T.; Feng, Q. L. *J. Cryst. Growth* **2003**, *258*, 402.

(271) Checa, A. G.; Okamoto, T.; Ramirez, J. *Proc. R. Soc. Lond. B.* **2006**, *273*, 1329.

(272) Dalbeck, P.; England, J.; Cusack, M.; Lee, M. R.; Fallick, A. E. *Eur. J. Mineral.* **2006**, *18*, 601.

(273) Lorens, R. B.; Bender, M. L. *Geochim. Cosmochim. Acta* **1980**, *44*, 1265.

(274) Doerner, H. A.; Hoskins, W. M. *J. Am. Chem. Soc.* **1925**, *47*, 662.

(275) Vander Putten, E.; Dehairs, F.; Keppens, E.; Baeyens, W. *Geochim. Cosmochim. Acta* **2000**, *64*, 997.

(276) Rosenberg, G. D.; Hughes, W. W. *Lethaia* **1991**, *24*, 83.

(277) Rosenberg, G. D.; Hughes, W. W.; Parker, D. L.; Ray, P. D. *Am. Malacol. Bull.* **2001**, *16*, 251.

(278) Kralj, D.; Kontrec, J.; Brecevic, L.; Falini, G.; Noethig-Laslo, V. *Chem. Eur. J.* **2004**, *10*, 1647.

(279) Dauphin, Y.; Cuif, J.-P.; Doucet, J.; Salome, M.; Susini, J.; Williams, C. T. *Marine Biology* **2003**, *142*, 299.

(280) Dauphin, Y.; Cuif, J. P.; Salome, M.; Susini, J.; Williams, C. T. *Anal. Bioanal. Chem.* **2006**, *386*, 1761.

(281) Kampschulte, A.; Strauss, H. *Chem. Geol.* **2004**, *204*, 255.

(282) Kontrec, J.; Kralj, D.; Brecevic, L.; Falini, G.; Fermani, S.; Noethig-Laslo, V.; Mirosavljevic, K. *Eur. J. Inorg. Chem.* **2004**, *2004*, 4579.

(283) Freitas, P. S.; Clarke, L. J.; Kennedy, H.; Richardson, C. A.; Abrantes, F. *Geochim. Cosmochim. Acta* **2006**, *70*, 5119.

(284) Lorrain, A.; Gillikin, D. P.; Paulet, Y. M.; Chauvaud, L.; Le Mercier, A.; Navez, J.; Andre, L. *Geology* **2005**, *33*, 965.

(285) Checa, A. G.; Jimenez-Lopez, C.; Rodriguez-Navarro, A.; Machado, J. P. *Marine Biology* **2007**, *150*, 819.

(286) Wanamaker, A. D. J.; Kreutz, K. J.; Borns, H. W. J.; Introne, D. S.; Feindel, S.; Funder, S.; Rawson, P. D.; Barber, B. J. *Paleoceonography* **2007**, *22*, . doi:10.1029/2006PA001352.

(287) Lécuyer, C.; Reynard, B.; Martineau, F. *Chem. Geol.* **2004**, *213*, 293.

(288) Schone, B. R.; Giere, O. *Deep-Sea Res. Part I Oceanogr. Res. Pap.* **2005**, *52*, 1896.

(289) Tada, Y.; Wada, H.; Miura, H. *Antarct. Sci.* **2006**, *18*, 111.

(290) Scheffel, A.; Gruska, M.; Faivre, D.; Linaroudis, A.; Graumann, P. L. J. M., P.; Schüler, D. *Nature* **2006**, *440*, 110.

(291) Parkinson, D. The use of stable isotope determinations from brachiopod shells in environmental reconstruction. Ph.D. Thesis, University of Glasgow, Glasgow, Scotland, United Kingdom, 2004; p 299.

CR078270O